U.S. Department
of Transportation
Federal Railroad
Administration

Office of Research,
Development and Technology
Washington, DC 20590

Ballast Fouling Measurement Tool – Phase III

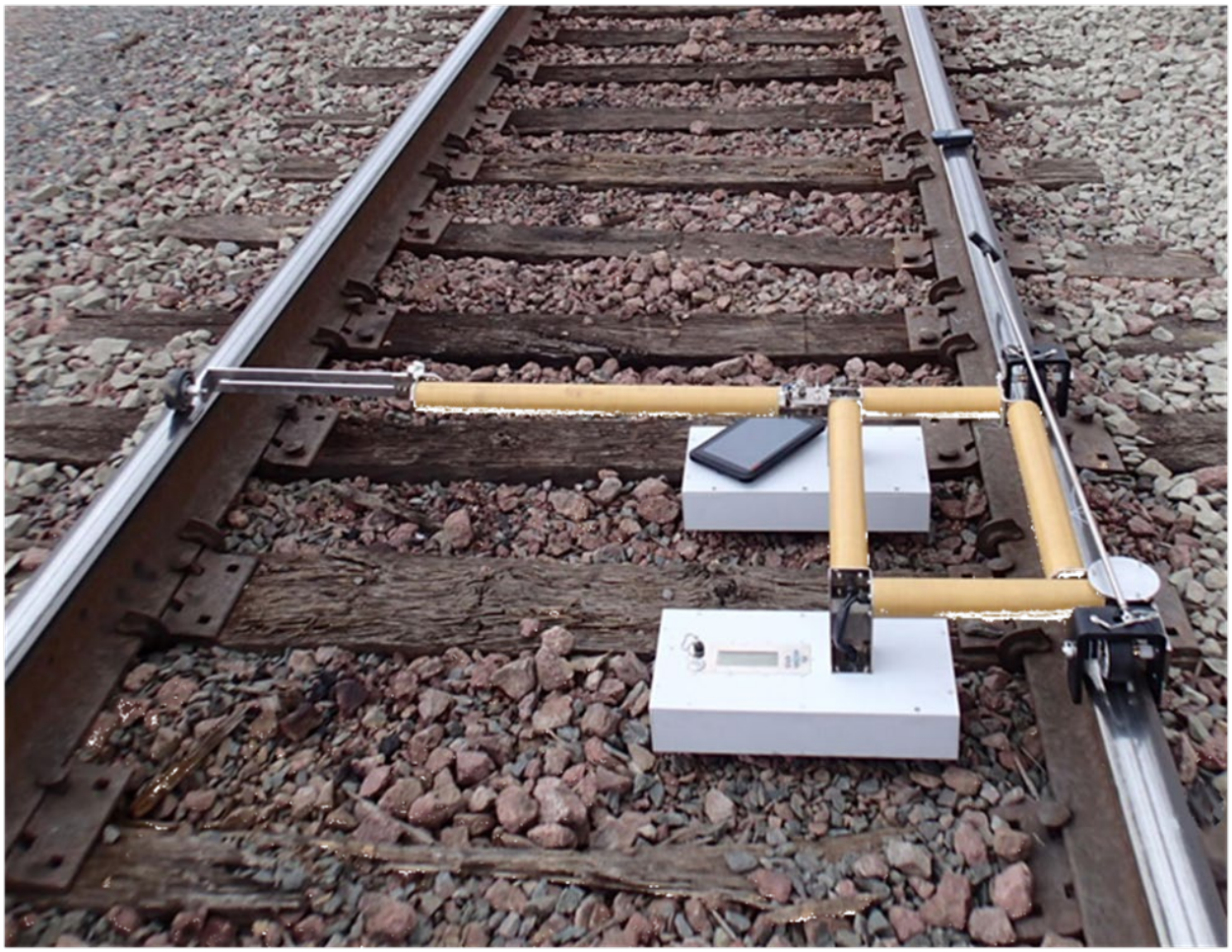

NOTICE

This document is disseminated under the sponsorship of the Department of Transportation in the interest of information exchange. The United States Government assumes no liability for its contents or use thereof. Any opinions, findings and conclusions, or recommendations expressed in this material do not necessarily reflect the views or policies of the United States Government, nor does mention of trade names, commercial products, or organizations imply endorsement by the United States Government. The United States Government assumes no liability for the content or use of the material contained in this document.

NOTICE

The United States Government does not endorse products or manufacturers. Trade or manufacturers' names appear herein solely because they are considered essential to the objective of this report.

REPORT DOCUMENTATION PAGE

Form Approved
OMB No. 0704-0188

1. AGENCY USE ONLY (Leave blank)	2. REPORT DATE	3. REPORT TYPE AND DATES COVERED
	28 August, 2024	Technical Report, January 2018–April 2019

4. TITLE AND SUBTITLE
Ballast Fouling Measurement Tool – Phase III

5. FUNDING NUMBERS

6. AUTHOR(S)
Charles P. Oden, ORCID #0000-0002-1510-4369
Carlton L. Ho, ORCID #0000-0002-151 0-4369
Aaron J. Rubin, ORCID #0000-0002-6512-5360

7. PERFORMING ORGANIZATION NAME(S) AND ADDRESS(ES)
Earth Science Systems, LLC
11485 W. I-70 Frontage Rd., Unit B
Wheat Ridge, CO 80033

8. PERFORMING ORGANIZATION REPORT NUMBER

9. SPONSORING/MONITORING AGENCY NAME(S) AND ADDRESS(ES)
U.S. Department of Transportation
Federal Railroad Administration
Office of Railroad Policy and Development
Office of Research, Development and Technology
Washington, DC 20590

10. SPONSORING/MONITORING AGENCY REPORT NUMBER
DOT/FRA/ORD-24/27

11. SUPPLEMENTARY NOTES
COR: Jay Baillargeon

12a. DISTRIBUTION/AVAILABILITY STATEMENT
This document is available to the public through FRA's eLibrary.

12b. DISTRIBUTION CODE

13. ABSTRACT (Maximum 200 words)
Researchers developed a second-generation RAdar Ballast Inspection Tool (RABIT) based on ground-penetrating radar (GPR) for use by track inspectors. This system is much lighter (26 lbs/11.8 kg) than its predecessor and is portable. It has a single bi-static antenna pair that straddles the tie, enabling the ballast properties under the tie to be measured. During a measurement, the RABIT rolls down the track and obtains average ballast properties over a span of 10 cribs, thereby reducing problems associated with local variability in ballast properties and tie geometry. Researchers collected measurements and ground truth data at 12 test track locations and 84 in-service track locations. The research team trained a neural network to map GPR waveforms to ballast fouling and moisture estimates. The correlation factor between the RABIT estimates and measured values determined from physical ballast samples was greater than 0.9.

14. SUBJECT TERMS
Ground-penetrating radar, ballast, fouling, moisture

15. NUMBER OF PAGES
49

16. PRICE CODE

17. SECURITY CLASSIFICATION OF REPORT	18. SECURITY CLASSIFICATION OF THIS PAGE	19. SECURITY CLASSIFICATION OF ABSTRACT	20. LIMITATION OF ABSTRACT
Unclassified	Unclassified	Unclassified	

NSN 7540-01-280-5500

Standard Form 298 (Rev. 2-89)
Prescribed by
ANSI Std. 239-18
298-102

METRIC/ENGLISH CONVERSION FACTORS

ENGLISH TO METRIC	METRIC TO ENGLISH
LENGTH (APPROXIMATE)	**LENGTH** (APPROXIMATE)
1 inch (in) = 2.5 centimeters (cm)	1 millimeter (mm) = 0.04 inch (in)
1 foot (ft) = 30 centimeters (cm)	1 centimeter (cm) = 0.4 inch (in)
1 yard (yd) = 0.9 meter (m)	1 meter (m) = 3.3 feet (ft)
1 mile (mi) = 1.6 kilometers (km)	1 meter (m) = 1.1 yards (yd)
	1 kilometer (km) = 0.6 mile (mi)
AREA (APPROXIMATE)	**AREA** (APPROXIMATE)
1 square inch (sq in, in^2) = 6.5 square centimeters (cm^2)	1 square centimeter (cm^2) = 0.16 square inch (sq in, in^2)
1 square foot (sqft, ft^2) = 0.09 square meter (m^2)	1 square meter (m^2) = 1.2 square yards (sqyd, yd^2)
1 square yard (sqyd, yd^2) = 0.8 square meter (m^2)	1 square kilometer (km^2) = 0.4 square mile (sq mi, mi^2)
1 square mile (sq mi, mi^2) = 2.6 square kilometers (km^2)	10,000 square meters (m^2) = 1 hectare (ha) = 2.5 acres
1 acre = 0.4 hectare (he) = 4,000 square meters (m^2)	
MASS - WEIGHT (APPROXIMATE)	**MASS - WEIGHT** (APPROXIMATE)
1 ounce (oz) = 28 grams (gm)	1 gram (gm) = 0.036 ounce (oz)
1 pound (lb) = 0.45 kilogram (kg)	1 kilogram (kg) = 2.2 pounds (lb)
1 short ton = 2,000 pounds (lb) = 0.9 tonne (t)	1 tonne (t) = 1,000 kilograms (kg)
	= 1.1 short tons
VOLUME (APPROXIMATE)	**VOLUME** (APPROXIMATE)
1 teaspoon (tsp) = 5 milliliters (ml)	1 milliliter (ml) = 0.03 fluid ounce (floz)
1 tablespoon (tbsp) = 15 milliliters (ml)	1 liter (l) = 2.1 pints (pt)
1 fluid ounce (floz) = 30 milliliters (ml)	1 liter (l) = 1.06 quarts (qt)
1 cup (c) = 0.24 liter (l)	1 liter (l) = 0.26 gallon (gal)
1 pint (pt) = 0.47 liter (l)	
1 quart (qt) = 0.96 liter (l)	
1 gallon (gal) = 3.8 liters (l)	
1 cubic foot (cu ft, ft^3) = 0.03 cubic meter (m^3)	1 cubic meter (m^3) = 36 cubic feet (cu ft, ft^3)
1 cubic yard (cu yd, yd^3) = 0.76 cubic meter (m^3)	1 cubic meter (m^3) = 1.3 cubic yards (cu yd, yd^3)
TEMPERATURE (EXACT)	**TEMPERATURE** (EXACT)
[(x-32)(5/9)] °F = y °C	[(9/5) y + 32] °C = x °F

QUICK INCH - CENTIMETER LENGTH CONVERSION

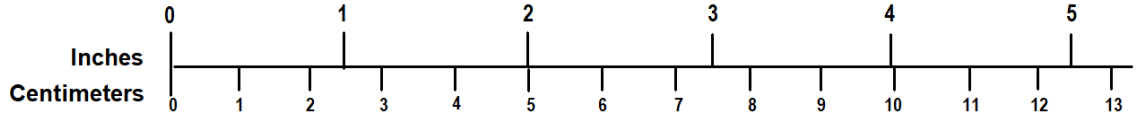

QUICK FAHRENHEIT - CELSIUS TEMPERATURE CONVERSION

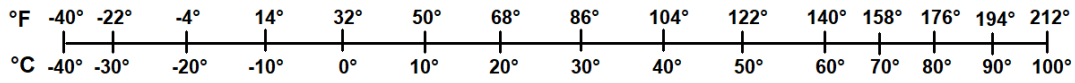

For more exact and or other conversion factors, see NIST Miscellaneous Publication 286, Units of Weights and Measures. Price $2.50 SD Catalog No. C13 10286

Updated 6/17/98

Acknowledgments

The authors acknowledge Hugh Thompson and Gary Carr (retired) of the U.S. Department of Transportation's Federal Railroad Administration and Ted Sussmann of the U.S. Department of Transportation's Volpe National Transportation Systems Center for their support, advice, and assistance during this activity. The authors also acknowledge BNSF Railway for providing access to revenue service track for measuring and collecting ballast samples.

Contents

Figures

Tables

Executive Summary

The Federal Railroad Administration (FRA) sponsored Earth Science Systems, LLC (ESS) to build a second-generation portable GPR system called the RAdar Ballast Inspection Tool (RABIT), which allows track inspectors to non-destructively assess in-situ ballast fouling and moisture conditions. In October 2018, researchers successfully demonstrated the prototype system at 12 test track locations, 84 in-service track locations within the BNSF Railway network, and at FRA's Transportation Technology Center (TTC). The test track fouling ranged from 0–75 percent and the moisture content ranged from 0–14.2 percent by weight. After the research team took RABIT measurements at these sites, they collected physical ballast samples and sent them to a laboratory to assess the actual fouling and moisture values. The team trained a neural network to map GPR waveforms of the assessed ballast fouling and moisture estimates. The correlation coefficient between the RABIT estimates and measured values determined from physical ballast samples was better than 0.9, and the mean squared error between estimated and measured values was less than 10 percent. Although initial tests succeeded, further testing is necessary to ensure that the neural network estimator has not been over-trained on site-specific features and that the algorithms are sufficiently robust and can be used throughout the in-service rail network. This report covers the third year of a three-year project.

The first prototype RABIT weighed 63 lbs (29 kg) and was larger and heavier than desired. This system contained a transmitting antenna, two receiving antennas operating at 450 MHz, and a second set of antennas with the same arrangement operating at 2 GHz. This system had antennas placed directly on the ballast surface to make "spot" measurements. Previous tests showed 1) significant variability on the GPR response from spot to spot, 2) that most of the information contained in the 2 GHz data could be obtained from the 450 MHz data, and 3) that the 450 MHz data provided valuable depth and thickness information that could not be obtained from the 2 GHz data. Therefore, ESS built the second-generation RABIT with only 500 MHz antennas, for which the transmitting antenna and first receiving antenna are located on the gage side of the rail and the second receiving antenna is placed on the field side of the rail. This unit incorporates a cart that can roll on the track, producing an average measurement over a defined number of cribs (e.g., 10 cribs), thereby reducing problems associated with local variability in ballast properties and tie geometry. To allow free movement along the track, the bottoms of the antennas were placed 2 inches above the ballast surface. Tests with the second-generation RABIT showed data from the receiving antenna located outside the rail had much poorer signal quality than the data from the inside receiver antenna. Therefore, ESS removed the outside antenna. Currently, the RABIT has only one transmitting antenna and one receiving antenna, making it more lightweight (26 lbs/11.8 kg) and portable.

The results were encouraging, showing that moisture and fouling can be successfully measured with non-invasive methods. Although the RABIT instrument and analysis routines have performed well in tests to date, the system needs continued verification, testing, and adjustments to demonstrate that it can be applied in most field conditions. For more background on this project, see the Phase I (FRA, 2014) and Phase II reports (FRA, 2024).

1. Introduction

1.1 Background

Ballast fouling is one of the primary causes of subsurface support structure degradation in railways. It lowers resistance to forces applied by the ties and reduces resilient modulus and energy absorption capacity (Selig and Waters, 1994). Previous research (FRA, 2014; Oden et al., 2017; Silvast, et al., 2010; Al-Qadi et al., 2007) has shown that ground-penetrating radar (GPR) is a promising technique for investigating the condition of railway ballast and subgrades.

This project seeks to develop, test, and demonstrate a non-invasive ballast inspection method that can be used by railroad track inspectors. During Phases I and II of this project (FRA, 2014,2024), Earth Science Systems, LLC (ESS) demonstrated that GPR data collected by the RABIT can be analyzed to provide useful estimates of ballast fouling and moisture. The aim of Phase III is to expand on this previous research and provide a quantitative assessment of ballast condition. ESS developed an instrument that makes the required measurements without disturbing or removing any ballast. In accordance with Federal Railroad Administration (FRA) recommendations, the developed instrument is lightweight (26 lbs/11.8 kg) and can be carried by one person. The instrument estimates the Selig fouling index (ref?) and moisture present in the ballast.

1.2 Objectives

The objectives of this phase of the project are provided below:

- Design a truly portable second-generation RABIT.
- Show that a single set of 500 MHz antennas is sufficient to provide robust estimates of ballast fouling and moisture content.
- Demonstrate that by taking continuous measurements over multiple cribs, local variations in ballast properties and tie geometry do not skew the readings.
- Demonstrate the strong correlation between ballast properties determined from tests of physical samples and estimates provided by the RABIT.
- Plan a field testing program that will demonstrate the value of the new tool and encourage adoption by the industry.
- Investigate the relationships of the properties measured by the RABIT to other properties, such as elastic modulus and yield strength.
- Conduct finite element modeling of track structures to relate ballast fouling and moisture to load deflections experienced by the track under load of passing trains.

1.3 Scope

This project examines the viability of using ground coupled GPR for ballast inspection. The research team intentionally did not consider air-coupled and mobile radar units that are operated from hi-rail vehicles, geometry cars, and other rolling stock. To create a portable instrument that one person can carry (a primary goal of the project), the team also limited the size of the array. A more complete picture of the ballast and sub-ballast can be obtained with an array of antennas spanning from one shoulder to the other, possibly spanning multiple cribs, but these large arrays are not portable by one person. Because the RABIT is designed to take localized measurements

of fouling and moisture, the researchers did not attempt to identify continuous subsurface structures that require measurements over length scales greater a few meters, such as continuous layer boundaries, ballast pockets, and clay lenses.

1.4 Overall Approach

This project was divided into three phases of work that each required approximately 1 year to complete. In Phase I, ESS built a prototype RABIT and tested it on a full-scale indoor track model. They designed the initial RABIT to make measurements at a single crib location. A physics-based (i.e., derived from Maxwell's equations, wave propagation, and electromagnetic properties of materials) analysis program was created to estimate ballast condition from the GPR data. The prototype was too heavy and bulky for one-person inspection efforts and, based on the results, there was significant variation in measured ballast properties from crib to crib.

For Phase II, ESS rebuilt the RABIT so that it had fewer antennas, was more lightweight, and could roll down the track to get an average reading over multiple cribs. They built an outdoor track with known ballast fouling conditions and used it to collect and analyze test data. The physics-based analysis was replaced with a neural network that was more robust to geometric variations, such as tie alignment in actual field conditions. The initial neural network results were encouraging, but it was clear that more testing was needed to validate the method.

The improved, lightweight RABIT used the latest GPR electronics. Three more field tests were conducted on revenue service railroad track. This provided 94 different test locations, each with different ballast conditions. At each test location, ESS collected a physical sample and tested it in the laboratory to provide ground truth. After updating the neural network training with data from these field sites, the correlation coefficient between the RABIT estimates and measured values determined from physical ballast samples was greater than 0.9 and the mean squared error between estimated and measured values was less than 10 percent. ESS created a finite element model (FEM) for initial investigations into the relationship between fouling, moisture, and the actual deflections experienced by a loaded track. Finally, a Track Inspector from FRA's Office of Safety, Region 7, evaluated the RABIT and offered valuable suggestions for improvement.

1.5 Organization of the Report

This report covers the design and construction of the basic technologies involved in the RABIT system. Section 2 discusses the background and hardware design of the portable GPR unit. Section 3 presents construction and testing of a test track as well as a summary of additional field testing efforts in revenue service and at TTC. Section 4 discusses data analysis and system assessment. Section 5 gives a step-by-step overview of the operation of the RABIT for conducting an inspection survey and summarizes the independent evaluation of the usability and portability by an FRA regional track inspector, including proposed improvements based on this feedback. Section 6 provides an overview of the finite element modeling used. Lastly, Section 7 summarizes findings, presents conclusions, and offers suggestions for further research. Each section is presented in the chronological order that the work was performed.

2. RABIT Hardware Design

The following sub-sections present the scientific background for the application of GPR technology for railroad ballast inspections as well as a detailed overview and associated technical discussion of the development and construction of the working prototype of the portable GPR unit used in this study.

2.1 GPR Response to Ballast Material

GPRs transmit temporally compact electromagnetic (EM) wavelets that travel through a subsurface medium along a direct or reflected wave path and arrive at the receiver after some delay and with some attenuation. When a radar's transmitting and receiving antennas are placed on or near the ground with a constant offset between them (i.e., a bi-static antenna configuration), a direct wave travels between the antennas through the air, another direct wave travels through the ground, and reflected waves occur when incident waves bounce off contrast between EM properties in the subsurface (or above the surface). With knowledge of the wave path and the measured travel time and attenuation, the EM properties of the media along the wave path can be deduced.

The attenuation of EM waves occurs when a medium absorbs energy and when the waves scatter out of the travel path. This scattering can be specular or diffuse. Specular scattering occurs when waves bounce off surfaces that are much larger than a wavelength (e.g., the bottom of a horizontal layer), and diffuse volume scattering occurs when the surfaces are smaller or similar to a wavelength (e.g., voids between the aggregate). All waves experience wavefront spreading where the amplitude falls off as r^{-2} from the transmitting antenna (where r is distance from the antenna).

The travel time of an EM wave depends on the wave velocity of the medium, which in turn depends on the dielectric constant (which can be frequency-dependent). The dielectric constant of ballast material depends on the type of aggregate material, the number of fines filling the voids, and the moisture content. In a layered medium, the travel time of a reflected wave recorded using a pair of antennas (one for transmitting and the other for receiving) at a fixed offset does not provide enough information to determine both layer thickness and wave velocity. However, if the dielectric constant can be estimated by other means (e.g., wave shape or attenuation versus frequency), then it is possible to estimate layer thicknesses.

The shape of the early waveforms that arrive before the reflected waves is a combination of the direct air waves and ground waves. These waveforms are complex and difficult to model from a physics-based approach (Oden, 2006); however, they do contain useful information and can be interpreted in a heuristic manner.

GPR surveys can be conducted over a wide range of frequencies (and wavelengths), but generally are performed in the 50 MHz to 2 GHz range. The EM wavelength in earth materials is mostly a function of moisture content but is also sensitive to fouling. For dry earth, the wavelengths at 50 MHz and 2 GHz are typically 118.1 inches and 3.0 inches (300 cm and 7.5 cm), respectively, and 47.2 inches and 1.2 inches (120 cm and 3 cm) for wet earth. At low frequencies, the penetration is good when conductivity is low, but the resolution is poor. At high frequencies the resolution is good, but diffuse volume scattering can cause significant attenuation. Volume scattering occurs when the particle size (aggregate or voids) is similar to a

wavelength. In general, there is a frequency window where GPR works well. At low frequencies, the attenuation (per wavelength) increases with increasing conductivity and decreasing frequency. At high frequencies, the attenuation increases with increasing aggregate or void size and with increasing electrical contrast between the aggregate and voids. Additionally, as frequency increases above 1 GHz, the attenuation increases due to the dielectric relaxation of water. As a result, GPR surveys are commonly operated within the 50 MHz to 2 GHz window.

2.2 RABIT Design and Prototype

ESS built the initial prototype RABIT to collect multi-offset data at both 2 GHz and 500 MHz. While this configuration provided a rich dataset, the unit proved too heavy and unwieldy. Test results showed that the 2 GHz data did not provide value that was not already achieved with the 500 MHz data. Therefore, the second-generation RABIT only had three 500 MHz antennas. This configuration provided a pair of antennas that straddled a tie and another antenna that straddled the rail. Further testing showed that the data from the antennas straddling the rail had a much poorer signal quality than the data from the tie straddling antennas. Consequently, the antenna outside the rail was removed to leave the system with only two antennas. The result is a much more lightweight and portable system (Figure 1 and Figure 2). The current weight of the unit is 26 lbs (11.8 kg), and the folded dimensions are 27 by 30 by 11 inches (68.6 by 76.2 by 27.9 cm).

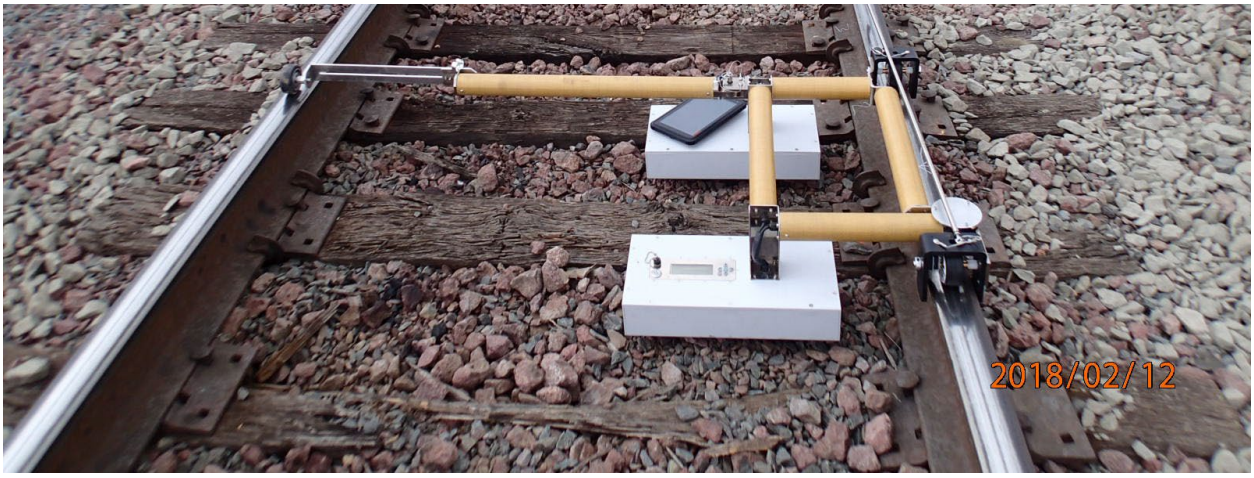

Figure 1. This photograph shows the RABIT deployed on an outdoor track with the antennas (the white boxes) straddling a tie and the frame resting on the track.

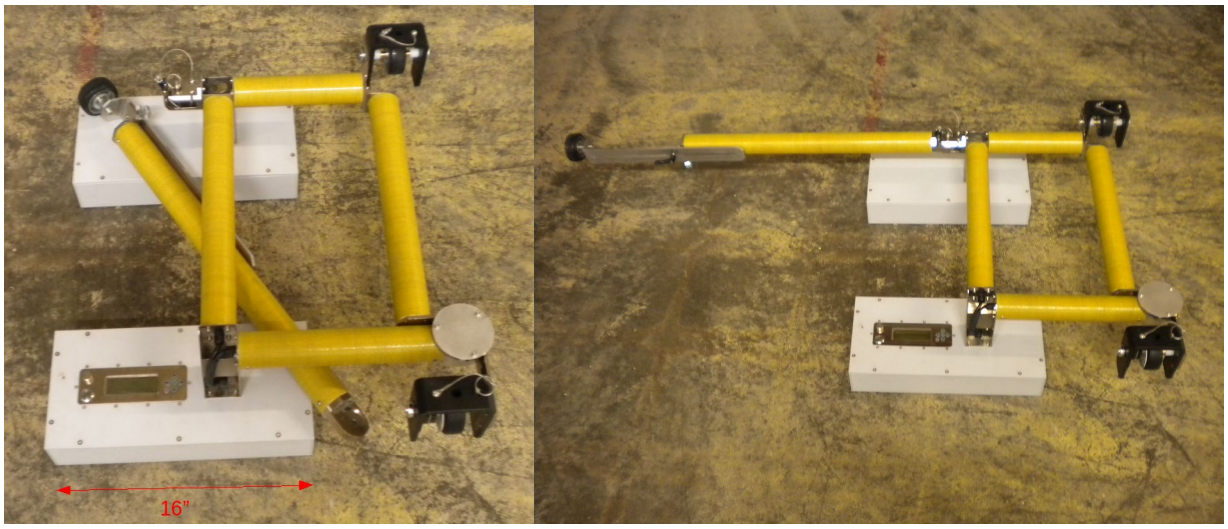

Figure 2. The final RABIT configuration is shown folded for transport (left) and with an extended outrigger (right). There is a wheel on the end of the outrigger and two wheels on the right side of the frame.

The RABIT has wheels that allow it to easily be pushed or pulled along the track, as shown in Figure 2. A push rod (not shown) attaches near the wheels on left to push or pull the unit. It was designed for a rail height of 7.625 inches (19.4 cm) with a 0.875-inch (2.2 cm) tie plate, a tie spacing of 19 inches (48.3 cm), and an adjustable outrigger to accommodate different track gages. It contains an internal battery that provides power for about 4 hours of continuous operation.

3. Field Tests

Over the course of this project, the ESS team took five 1-week field trips to test the RABIT on various tracks. In subsequent discussions, the datasets from these trips will be referred to as Group 1 through Group 5 data. The following sections describe the work done during each trip.

3.1 BNSF Technical Research and Development Facility (Topeka, KS)

During Phase II of this project, a test track with varying ballast conditions was built at BNSF Railway's Technical Research and Development facility in Topeka, KS. The test section was 60 feet long, divided into 15-foot sections, each with different fouling levels. The rail size was 136-lb AREA rail (rail height: 7 5/16 inches).

Figure 3. View of the test track to the northeast

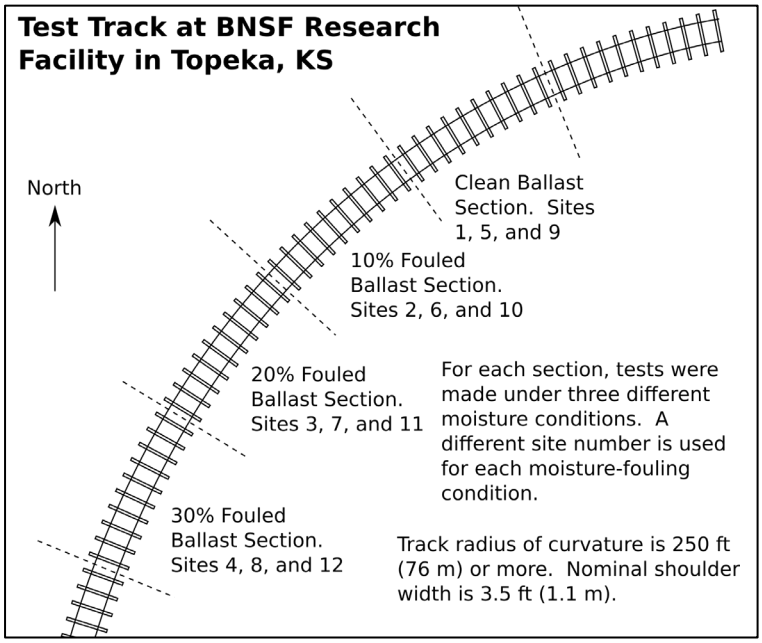

Figure 4. Test track layout diagram

During construction of the test track, the team made four ballast mixtures, each with a different fouling level (nominally 0 percent, 10 percent, 20 percent, and 30 percent by weight). Construction began with laying down and compacting ballast to a thickness of 17–25 inches (43.2–64.5 cm). The ties and rail were then laid. Finally, the ballast in the cribs was added and compacted with a hand-held tamper. The ballast below the ties was likely better compacted than the ballast between the ties. Ties were placed at a center-to-center spacing of approximately 18–20 inches (45.7–50.8 cm) with local variations of +/- 3 inches (7.6 cm).

The RABIT took measurements on the test track at three different moisture conditions, referred to as "low moisture," "mid moisture," and "high moisture" (see Table 1 for actual values). Controlling the moisture was more difficult on the outdoor track than the indoor track used for the Phase I of this project. ESS conducted field measurements over a 4-week period in June 2017 after numerous recent and heavy rainfall events. The first test at the mid-moisture level was conducted 2 days after a heavy rain. For the low-moisture level, the test track stood for 1 week without precipitation and drained before testing began. Ballast drying occurred slowly because the test track was built on clay-rich, water-saturated soil near the Kansas River that was not conducive to drainage, and because the ambient humidity was high. For the final high-moisture level, the test track was irrigated beyond field capacity, covered, and allowed to sit overnight to allow the moisture distribution to reach equilibrium.

Table 1. Values of RABIT measurements

Site	Shallow Moisture (%)	Shallow Fouling (%)	Deep Moisture (%)	Deep Fouling (%)	Notes
1	0.29	1.20	0.29	1.20	From nominally 0% fouled section. Allowed track to drain for 1 week following a rain event.
2	0.58	2.6	0.58	2.6	From nominally 10% fouled section. Allowed track to drain for 1 week following a rain event.
3	1.81	22.7	1.81	22.7	From nominally 20% fouled section. Allowed track to drain for 1 week following a rain event.
4	3.35	44.7	3.35	44.7	From nominally 30% fouled section. Allowed track to drain for 1 week following a rain event.
5	0.57	0.2	0.57	0.2	From nominally 0% fouled section. Initial field conditions after recent rain event.
6	1.25	3.10	1.25	3.10	From nominally 10% fouled section. Initial field conditions after recent rain event.
7	1.96	11.7	1.96	11.7	From nominally 20% fouled section. Initial field conditions after recent rain event.
8	4.56	35.8	4.56	35.8	From nominally 30% fouled section. Initial field conditions after recent rain event.
9	0.95	0.58	0.95	0.58	From nominally 0% fouled section. Irrigated to field capacity.
10	2.81	8.70	2.81	8.70	From nominally 10% fouled section. Irrigated to field capacity.
11	4.18	19.6	4.18	19.6	From nominally 20% fouled section. Irrigated to field capacity.
12	4.56	33.0	4.56	33.0	From nominally 30% fouled section. Irrigated to field capacity.

RABIT data were collected for each moisture condition by running the GPR system down each side of the entire 60-foot test track at walking speed using a trace sampling rate of 50 traces per

second. An A-scan waveform (i.e., a time series waveform of the received radar wave with the antennas at a single location) was manually extracted for each tie location (typical waveforms are shown in Figure 4; no range gain has been applied). In general, the peak amplitude of the wave decreases as fouling increases. The two traces in each plot are data from the left and right sides of the track. The variation between the left and right waveforms could be due to locally different ballast properties or due to environmental factors such as tie spacing.

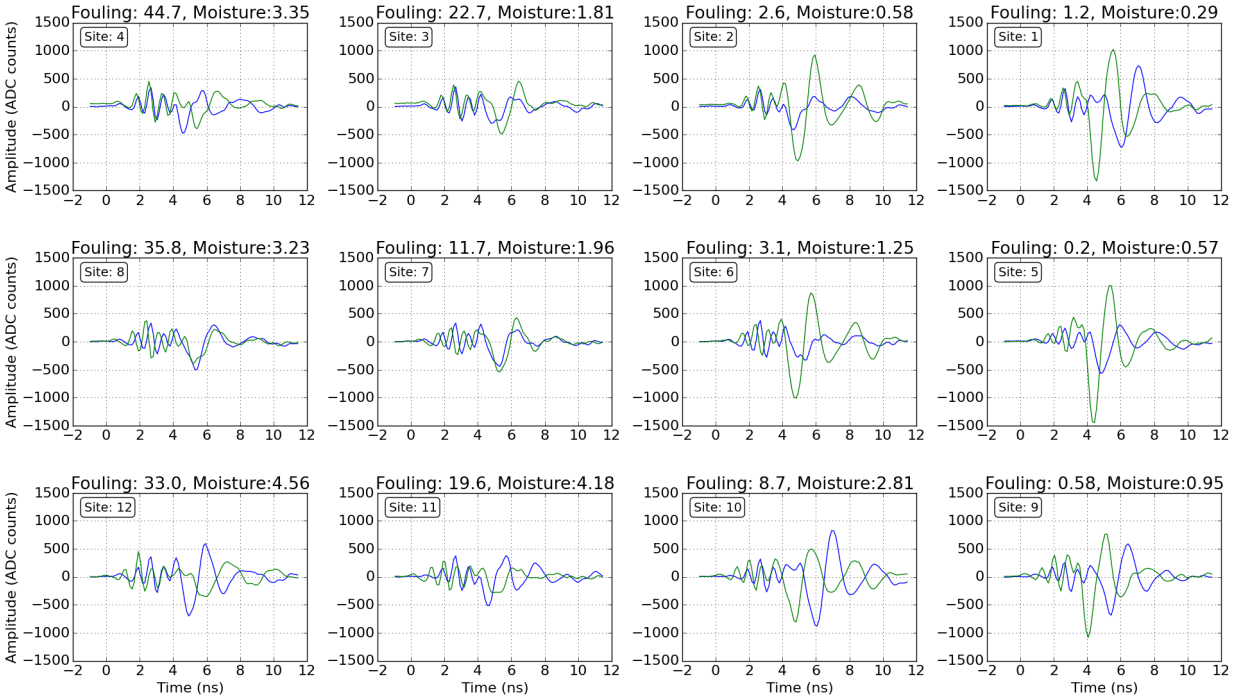

Figure 5. The graphs show waveforms for various ballast conditions for Group 1 collected at the BNSF Technical Research and Development Facility. Blue and green traces represent measurements taken on the left and right sides of track (respectively) on the gauge side of the rails.

To obtain the ground-truth properties of the ballast material, physical samples were extracted for each of the 12 fouling-moisture conditions represented in Figure 5 after the RABIT data were collected. For each sample, the team removed at least 165.3 lbs (75 kg) of ballast material from the crib, and the material was replaced using the previously prepared ballast mixtures. To preserve as much of the original track structure as possible, no more than one sample was taken from a given crib. Table 1 lists the properties determined by laboratory testing. The sampling process followed the method outlined by Yoo, et al. (1978). After removing the sample, the sample void was lined with a plastic sheet and filled with water. The volume of water needed to fill the void was considered equivalent to the volume of the sample. The samples were weighed before and after drying to determine moisture content in accordance with ASTM D2216-05 (ASTM, 2007). The dry samples were then sieved to determine the grain-size distribution in accordance with ASTM D6913-04 (ASTM, 2008). The actual fouling values differed from the targeted 0, 10, 20, and 30 percent fouling levels, which could have been due to insufficient control during the construction process. However, ESS observed significant spatial variability in fouling and moisture levels in other experiments conducted during Phase I and Phase II of this project.

The goal of the experiments at this site was to collect a dataset suitable for training algorithms that would estimate ballast condition. The collected data did have some non-ideal aspects and differences from previous field outings that should be considered when training and calibrating the ballast condition algorithms.

1. By observing the soil type at the site and noting that the location was very close (about 200 feet) to the Kansas River, researchers concluded that the sub-ballast was likely moist and clay rich. This site may not represent typical in-service track conditions.
2. The laboratory analysis of the physical samples did not divide the sample into shallow and deep sub-samples, as was done for the subsequent field trips. Consequently, the same fouling and moisture values were used for both shallow and deep ground-truth conditions.
3. When testing the physical samples for grain size distribution, a #200 screen was not used (as was used with samples from the other field outings). The standard Selig fouling index requires measuring the sample fraction that passes the #4 screen and the #200 screen. For these samples, researchers assumed that there was no material passing the #200 screen.
4. The tie spacing and alignment were not uniform. This may be similar to mainline track at other locations.
5. The field work was conducted in early summer when there were frequent thunderstorms. Since this was an outdoor site, the team could not measure the response to very dry conditions.
6. In many cases, there were marked differences between the waveforms on the left and right side of the track (see Figure 5), which indicates heterogeneity.
7. For each ballast condition, RABIT measurements were collected with the instrument straddling eight different ties. There was only one physical sample taken for each ballast condition.

3.2 BNSF Railway (Phoenix, AZ)

As Phase III of the project commenced, the research team made a field trip to Phoenix, AZ to collect more RABIT data and ground-truth samples using the procedures outlined above. The team visited various revenue service track sites within about a 60-mile radius of Phoenix with the goal of collecting data for a wide range of ballast conditions (i.e., from clean to dirty conditions). The trip occurred in February 2018, and there were a few heavy rains during the 1-week outing. Typical waveforms are shown in Figure 6 (no range gain has been applied). In general, the peak amplitude of the wave decreases as fouling increases. Either 132- or 136-lb AREA rails were installed at these sites Researchers extracted a physical sample at each test location that filled two 5-gallon buckets. One bucket was filled with ballast material from a depth of 6–8 inches (15.24–20.32 cm) and the second bucket was filled with deeper material from 14–16-inch depths (35.56–40.64 cm). The samples were weighed before and after drying to determine moisture content in accordance with ASTM D2216-05 (ASTM, 2007). The dry samples were then sieved to determine the grain-size distribution in accordance with ASTM D6913-04 (ASTM, 2008). The results are listed in Table 2 below.

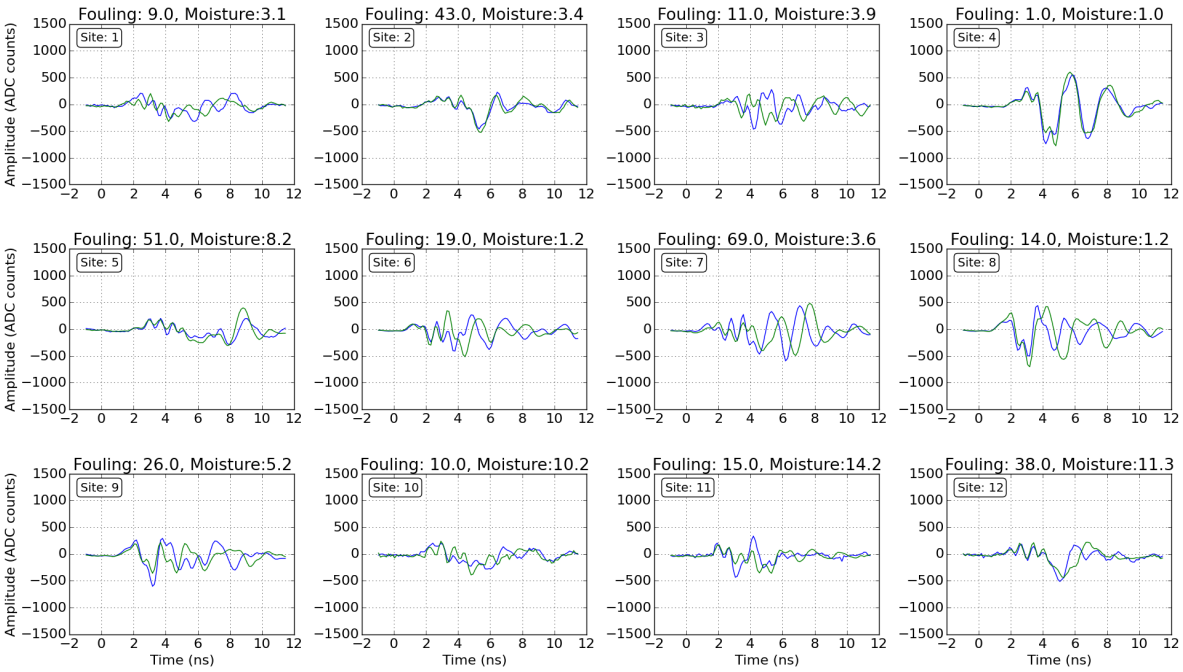

Figure 6. The figure shows waveforms for various ballast conditions for Group 2 on various BNSF Railway tracks near Phoenix, AZ. The blue and green traces represent measurements from left and right sides of track (respectively) on the gage side of the rails.

Table 2. The table shows fouling and moisture values from the Phoenix, AZ, test sites.

Site	Shallow Moisture (%)	Shallow Fouling (%)	Deep Moisture (%)	Deep Fouling (%)
1	3.1	9.0	5.6	34.0
2	3.4	43.0	3.9	47.0
3	3.9	11.0	6.6	39.0
4	1.0	1.0	1.7	15.0
5	8.2	51.0	9.8	64.0
6	1.2	19.0	3.1	48.0
7	3.6	69.0	5.5	75.0
8	1.2	14.0	3.3	30.0
9	5.2	26.0	5.2	30.0
10	10.2	10.0	7.7	37.0
11	14.2	15.0	10.0	32.0
12	11.3	38.0	7.0	55.0
13	6.8	4.0	8.1	7.0
14	13.5	49.0	12.2	64.0

As with previous field trips, the goal was to collect a dataset suitable for training algorithms that would estimate ballast condition. The collected data did have some non-ideal aspects and differences from previous field outings that should be considered when training and calibrating the ballast condition algorithms.

1. For this trip, ESS installed an embedded computer and receiver electronics on the RABIT. The amplitude response of the new electronics is slightly different than that of the older system, and the data have been adjusted to compensate for the difference in response.

2. The RABIT was designed for use on 132-lb AREA rail (rail height: 7 1/8 inches), 136-lb AREA rail (rail height: 7 5/16 inches), or 141-lb AREA rail (rail height: 7 5/8 inches), which produced an antenna ground clearance of 3.25–3.75 inches. The rail in the surveyed locations was either 132- or 136-lb AREA rail. In practice, the combination of railhead wear and tie plate seating reduced the clearance to about 2 inches above the tie. In some cases, this caused the RABIT to skid on ballast particles that rested on top of the ties.
3. In most locations, the top 2 inches of cribs were not filled. In some locations, the top 4 inches were not filled.
4. In some cases, there were marked differences between the waveforms on the left and right side of the track (see Figure 6). This indicates heterogeneity.
5. For each test site, the RABIT collected measurements with the instrument straddling 10 different ties. Researchers only obtained two physical samples for each test site, at two different depths within the same crib.

3.3 BNSF Railway (Kansas City, MO)

The team made a field trip to the Kansas City, MO area to collect more RABIT data and ground-truth samples using the procedures outlined above. Researchers visited various revenue service track sites within about a 60-mile radius of Kansas City, with the goal of collecting data for a wide range of ballast conditions (i.e., from clean to dirty conditions). The trip happened in May 2018, and there were a few heavy rains during the 1-week outing. Typical waveforms are shown in Figure 7 (no range gain has been applied).

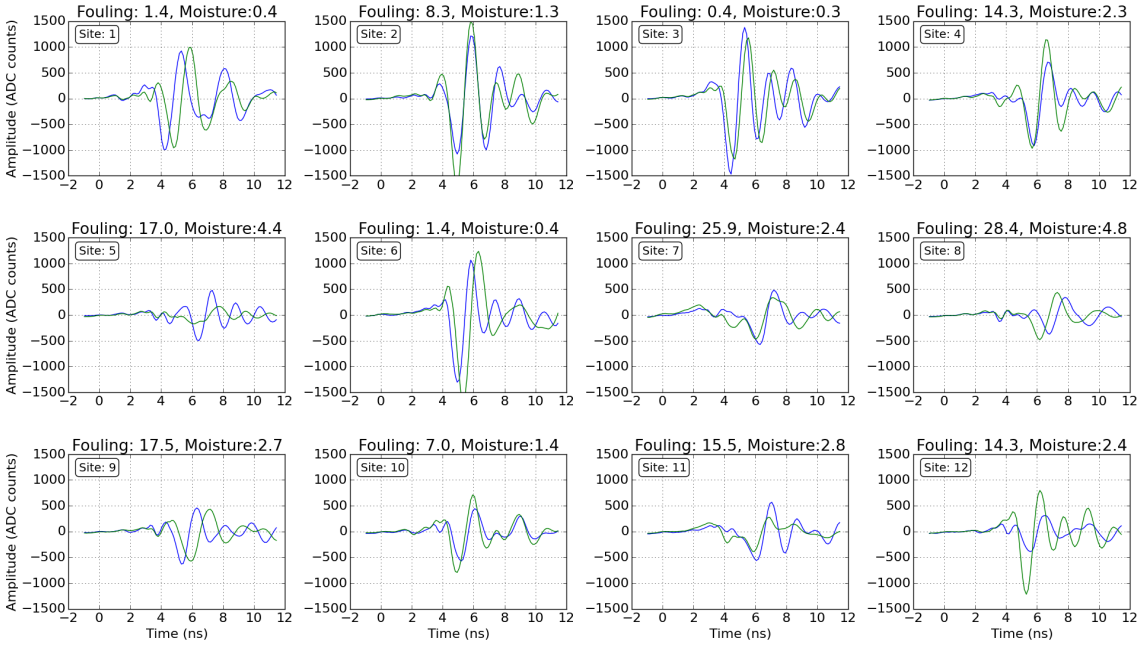

Figure 7. The figure shows waveforms for various ballast conditions for Group 3 on various BNSF Railway tracks near Kansas City, MO. Blue and green traces represent measurements taken on the left and right sides of track (respectively) on the gage side of the rails.

Either 132- or 136-lb AREA rail were installed at these sites. The team extracted a physical sample at each test location that filled two 5-gallon buckets. One bucket was filled with ballast material from a depth of 6–8 inches (15.24–20.32 cm) and the second bucket was filled with deeper material from depths extending to 14-16 inches (35.56–40.64 cm). The samples were weighed before and after drying to determine moisture content in accordance with ASTM D2216-05 (ASTM, 2007). The dry samples were then sieved to determine the grain-size distribution in accordance with ASTM D6913-04 (ASTM, 2008). The results are in Table 3.

Table 3. Fouling and moisture values from the Kansas City, MO test sites

Site	Shallow Moisture (%)	Shallow Fouling (%)	Deep Moisture (%)	Deep Fouling (%)	Notes
1	0.4	1.4	7.5	29.5	Top 0–3” of cribs not filled.
2	1.3	8.3	3.6	13.5	Top 0–2” of cribs not filled.
3	0.3	0.4	0.3	1.4	Top 0–2” of cribs not filled.
4	2.3	14.3	5.5	35.3	Top 0–3” of cribs not filled.
5	4.4	17.0	0.8	6.5	Top 1–3” of cribs not filled.
6	0.4	1.4	1.3	6.3	Top 0–1” of cribs not filled.
7	2.4	25.9	4.2	17.9	Top 0–1” of cribs not filled.
8	4.8	28.4	5.9	37.5	Top 0–2” of cribs not filled.
9	2.7	17.5	3.7	25.6	Top 1–3” of cribs not filled.
10	1.4	7.0	3.6	21.7	Top 2–6” of cribs not filled.
11	2.8	15.5	4.0	24.7	Top 2–6” of cribs not filled.
12	2.4	14.3	6.9	36.7	Top 0–1” of cribs not filled.
13	2.0	11.9	3.6	27.0	Top 1–2” of cribs not filled.
14	2.4	20.1	12.2	64.4	Top 1–2” of cribs not filled. Lab test results missing or inconsistent. Removed from analysis.
15	2.7	17.5	3.7	34.1	Top 1–3” of cribs not filled.
16	7.3	59.8	8.1	72.2	Top 1–2” of cribs not filled.
17	N/A	N/A	18.3	51.8	Top 0–3” of cribs not filled. Lab test results missing or inconsistent. Removed from analysis.
18	2.6	24.5	3.6	32.0	Top 1–3” of cribs not filled.
19	3.7	44.5	4.0	42.3	Top 1–2” of cribs not filled. Lab test results missing or inconsistent. Removed from analysis.

As with previous field trips, the goal was to collect a dataset suitable for training algorithms that would estimate ballast condition. The collected data did have some non-ideal aspects and differences from previous field outings that should be considered when training and calibrating the ballast condition algorithms.

1. For this trip, ESS installed a next-generation receiver circuit board. The amplitude response of the new electronics is slightly different than that of the older system, and the data have been adjusted to compensate for the difference in response.
2. There were inconsistencies in the results from the testing lab in Kansas City that processed the physical samples. This included missing results for some samples and multiple results reported for other samples. As a result, data could only be used from 16 of the 19 test locations. These inconsistencies also increased the probability of incorrect reporting on the 16 good sample locations.

3. Many of the cribs were not filled to the tops of the ties.
4. The RABIT was designed for use on 132-lb AREA rail (rail height: 7 1/8 inches), 136-lb AREA rail (rail height: 7 5/16 inches), or 141-lb AREA rail (rail height: 7 5/8 inches), which gave a clearance of 3.25 to 3.75 inches. The rail in the surveyed locations was either 132- or 136-lb AREA rail. In practice, the combination of railhead wear and tie plate seating reduced the clearance to about 2 inches above the tie. In some cases, this caused the RABIT to skid on ballast particles that rested on top of the ties.
5. In some cases, there were marked differences between the waveforms on the left and right side of the track (see Figure 7). This was an indication of ballast heterogeneity.
6. For each test site, the RABIT collected measurements with the instrument straddling 10 different ties. Only two physical samples were taken for each test site, at two different depths within the same crib.

3.4 BNSF Railway (Topeka, KS)

The team made a field trip to Topeka, KS to collect more RABIT data and ground-truth samples using the procedures outlined above. They visited various revenue service track sites within an approximate 60-mile radius of Topeka with the goal of collecting data for a wide range of ballast conditions (i.e., from clean to dirty conditions). The trip was made in June 2018, and there were a few heavy rains during the 1-week outing. Figure 8 shows typical waveforms; no range gain has been applied. The rail size installed at these sites was either 132- or 136-lb AREA rail unless otherwise noted. Researchers extracted a physical sample at each test location that filled two 5-gallon buckets. One bucket was filled with ballast material from a depth of 6–8 inches (15.24–20.32 cm) and the second bucket was filled with material from 14–16-inch depths (35.56–40.64 cm). The samples were weighed before and after drying to determine moisture content in accordance with ASTM D2216-05 (ASTM, 2007). The dry samples were then sieved to determine the grain-size distribution in accordance with ASTM D6913-04 (ASTM, 2008). The results are listed in Table 4 below.

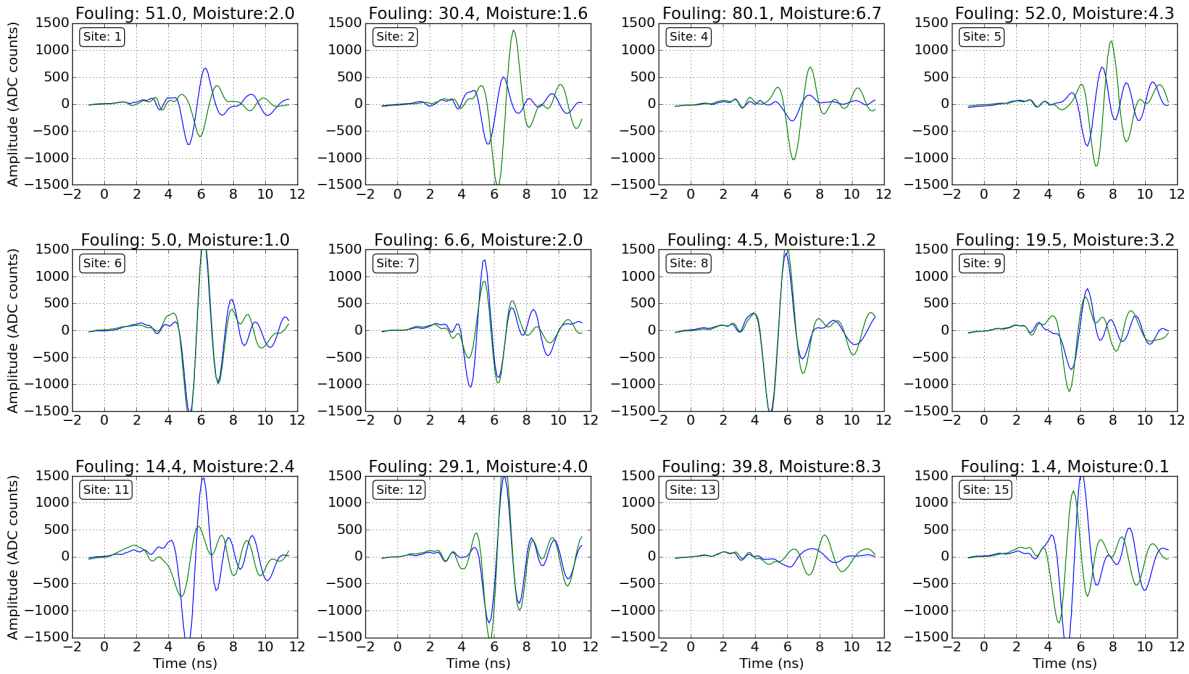

Figure 8. The graphs show waveforms for various ballast conditions for Group 4 on various BNSF Railway tracks near Topeka, KS. Blue and green traces represent measurements taken on the left and right sides of track (respectively) on the gage side of the rails.

Table 4. Fouling and moisture values from the Topeka 2018 test sites

Site Number	Shallow Moisture (%)	Shallow Fouling (%)	Deep Moisture (%)	Deep Fouling (%)	Notes
1	2.0	51.0	2.8	47.5	
2	1.6	30.4	2.3	36.2	
3	58.2	0.0	0.7	1.6	Lab test results missing or inconsistent. Removed from analysis.
4	6.7	80.1	7.6	93.3	
5	4.3	52.0	6.0	49.9	
6	1.0	5.0	1.8	11.7	
7	2.0	6.6	2.4	9.1	
8	1.2	4.5	2.8	17.4	
9	3.2	19.5	3.5	18.8	
10	0.8	1.4	3.2	33.2	Lab test results missing or inconsistent. Removed from analysis.
11	2.4	14.4	3.3	25.7	
12	4.0	29.1	3.6	31.0	
13	8.3	39.8	9.1	44.0	
14	0.4	6.0	6.0	23.0	Lab test results missing or inconsistent. Removed from analysis.
15	0.1	1.4	1.1	6.6	
16	0.6	1.4	1.2	2.8	
17	0.8	0.4	0.9	1.5	
18	3.0	14.2	4.1	22.8	
19	8.7	14.1	6.0	23.0	
20	0.8	1.3	0.3	1.7	
21	8.9	58.9	6.8	64.3	Rail type: 115-lb AREA rail
22	0.5	3.2	0.8	3.2	Rail type: 115-lb AREA rail

As with previous field trips, the goal was to collect a dataset suitable for training algorithms to estimate ballast condition. The collected data did have some non-ideal aspects that should be considered when training and calibrating the ballast condition algorithms:

1. There were inconsistencies in the results from the testing lab in Kansas City that processed the physical samples. This included missing results for some samples and multiple results reported for other samples. As a result, data could only be used from 19 of the 22 test locations. These inconsistencies also increased the probability of incorrect reporting on the 19 good sample locations.
2. The RABIT was designed for use on 132-lb AREA rail (rail height: 7-1/8 inches), 136-lb AREA rail (rail height: 7-5/16 inches), or 141-lb AREA rail (rail height: 7-5/8 inches), which gave a clearance of 3.25 to 3.75 inches. The rail in the surveyed locations was either 132- or 136-lb AREA rail. In some locations (see notes above), the rail type was 115-lb AREA rail (rail height: 6-5/8 inches). In practice, the combination of rail head wear and tie plate seating reduced the clearance to about 2 inches above the tie.
3. In some cases, there were marked differences between the waveforms on the left and right side of the track (see Figure 8). This indicated heterogeneity.
4. For each test site, the RABIT collected measurements with the instrument straddling 10 different ties. Only two physical samples were taken for each test site, at two different depths within the same crib.

3.5 Transportation Technology Center (Pueblo, CO)

The team made a field trip to the FRA's Transportation Technology Center near Pueblo, CO to collect more RABIT data and ground-truth samples using the procedures outlined above. The work was done on the High Tonnage Loop of the Facility for Accelerated Service Testing (FAST). They made the trip in October 2018, and there was drizzle to light rain during the entire 1-week outing. Figure 9 shows typical waveforms after being multiplied by a scaling factor of three (see discussion below). The rail size installed at these sites was either 136- or 141-lb AREA rail. Researchers extracted a physical sample at each test location that filled two 5-gallon buckets. One bucket was filled with ballast material from a depth of 6–8 inches (15.24–20.32 cm), and the second bucket was filled with material from depths extending to 14–16 inches (35.56–40.64 cm). The samples were weighed before and after drying to determine moisture content in accordance with ASTM D2216-05 (ASTM, 2007). The dry samples were then sieved to determine the grain-size distribution in accordance with ASTM D6913-04 (ASTM, 2008). The results are listed in Table 5 below.

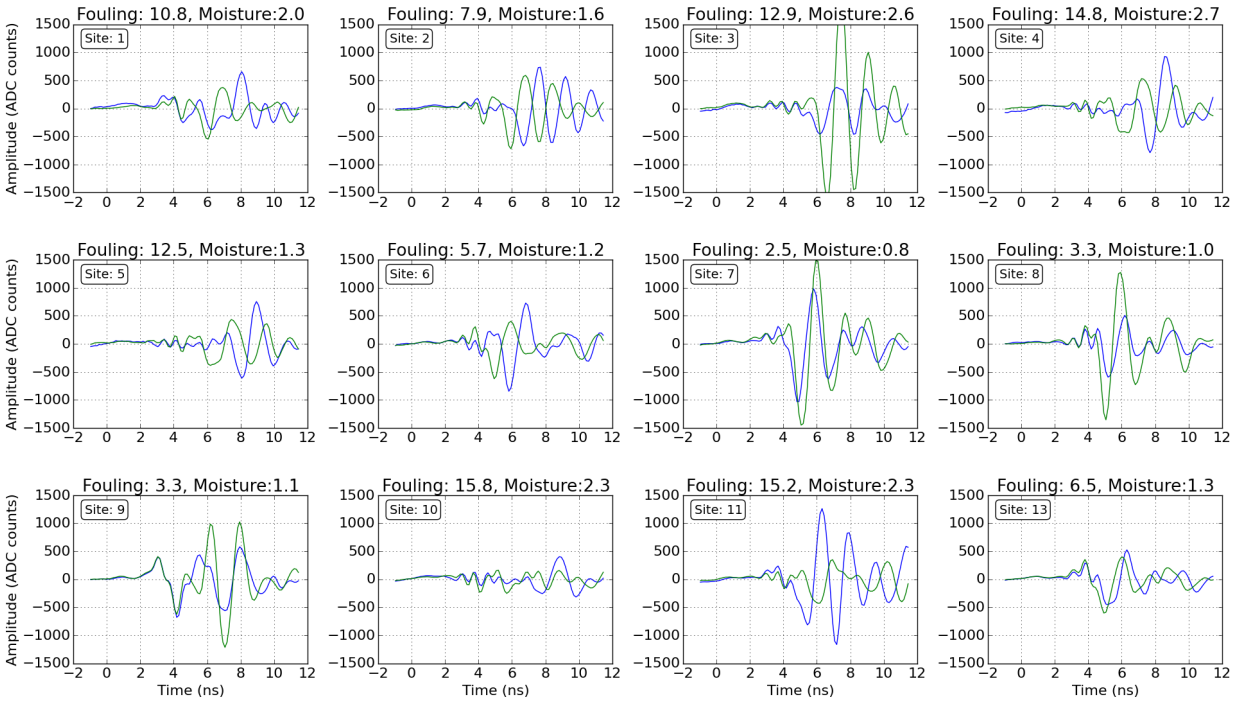

Figure 9. The graphs show waveforms for various ballast conditions for Group 5 on various TTC tracks near Pueblo, CO. Blue and green traces represent measurements taken on the left and right sides of track (respectively) on the gage side of the rails.

Table 5. Fouling and moisture values from the Pueblo test sites

Site Number	Shallow Moisture (%)	Shallow Fouling (%)	Deep Moisture (%)	Deep Fouling (%)	Notes
1	2.0	10.8	2.5	19.1	
2	1.6	7.9	2.4	16.8	
3	2.6	12.9	2.7	19.4	
4	2.7	14.8	3.4	26.5	
5	1.3	12.5	2.5	19.1	
6	1.2	5.7	2.0	14.1	
7	0.8	2.5	0.8	3.9	
8	1.0	3.3	2.1	15.2	
9	1.1	3.3	1.3	4.8	
10	2.3	15.8	3.6	25.8	
11	2.3	15.2	3.2	26.1	
12	2.1	12.7	2.0	12.9	Corrupt data file
13	1.3	6.5	1.2	6.9	
14	0.8	3.3	1.1	5.6	
15	1.1	5.0	1.8	13.5	
16	2.6	14.0	3.2	19.9	
17	0.9	2.0	1.2	3.8	
18	2.6	15.9	3.3	17.6	
19	1.7	2.6	1.7	3.5	
20	1.2	8.7	1.9	14.6	
21	2.1	15.7	2.0	15.9	
22	0.6	2.8	0.7	3.6	
23	1.4	9.4	2.1	16.5	
24	1.5	14.2	2.0	16.5	
25	1.0	5.7	1.5	10.6	
26	0.8	2.8	1.0	4.5	
27	0.8	7.5	1.0	3.8	

As with previous field trips, the goal was to collect a dataset suitable for training algorithms that would estimate ballast condition. The collected data did have some non-ideal aspects and differences from previous field outings that should be considered when training and calibrating the ballast condition algorithms:

1. For this trip, ESS added a GPS receiver to the RABIT, enabling the physical location to be recorded for each survey.
2. Although the RABIT is designed to be watertight, the sealing gasket on the antennas was inadvertently left out on final assembly. Midway through the first day of field work, the team realized that the antennas were filling with rainwater. At this point, work ceased for the day and the RABIT was disassembled and inspected. The antennas contain carbon loaded foam, which had become water-saturated, but the rest of the unit appeared to be in working order. The foam components of the antenna were dried overnight, and the RABIT was re-assembled; work resumed the following day.
3. After the field work was finished, ESS examined the waveform data and found substantially less amplitude than the previous file outings. The RABIT was examined and tested in the ESS laboratory and found to be in working order. Nevertheless, there were questions regarding whether the RABIT was operating properly and whether the data were valid.

4. Before analyzing the data from this field outing, ESS multiplied the waveform data by a factor of three so that the amplitude of the clean ballast waveforms was comparable to that from other field outings. There is no scientific or engineering basis for doing this.
5. The RABIT was designed for use on rail sizes 132-lb AREA rail (rail height: 7-1/8inches), 136-lb AREA rail (rail height: 7-5/16 inches), or 141-lb AREA rail (rail height: 7-5/8 inches), which gave a clearance of 3.25 to 3.75 inches. The rail in the surveyed locations was either 136- or 141-lb AREA rail.
6. In many cases, there are marked differences between the waveforms on the left and right side of the track (see Figure 9). This is an indication of heterogeneity.
7. For each test site, the RABIT collected measurements with the instrument straddling 10 different ties. Only two physical samples were taken for each test site, at two different depths within the same crib.

3.6 Comparison between Field Datasets

In the subsequent discussions, the data from the field outings will be referred to by group number:

- Group 1: Topeka, KS, June 2017
- Group 2: Phoenix, AZ, February 2018
- Group 3: Kansas City, KS, May 2018
- Group 4: Topeka, KS, June 2018
- Group 5: Pueblo, CO, October 2018

One reason for going to these different locations was to collect a dataset that was highly varied in terms of location-specific conditions other than ballast properties, or non-intrinsic ballast-variations (NBV). When knowledge was available about these conditions, it has been noted in the preceding sections. These location specific NBVs can change the waveforms recorded by the RABIT, and the analysis routines should be able to accommodate these changing conditions. This will be discussed further in the next section.

4. RABIT Data Analysis

The following sub-sections describe the analyses from field data Groups 1–5 and their results in detail. This consists of the full waveform and waveform attributes analyses and the neural network development, training, and verification. The last sub-section investigates the relationship between moisture and fouling of railroad ballast material.

4.1 Background

The goal of the data analysis was to provide real-time feedback to RABIT operators in the field, and to accurately estimate ballast fouling and moisture. A secondary goal was to measure ballast thickness. One method to measure thickness involves measuring the time it takes a wave to travel from the RABIT down through the ballast, reflect off the bottom, and travel back up to the RABIT. This method only works when there is a sharp contrast between the ballast and sub-ballast to provide a clear reflection. Oftentimes, however, this transition is gradational, and no clear reflection is evident. An approach that works in all situations is to measure ballast conditions at several fixed depths of investigation. To implement this approach, ESS made one set of estimator routines to predict shallow ballast properties (0–8 inches or 0–20 cm) and another set to predict deeper properties (8–16 inches or 20–40 cm). These estimators were trained using laboratory measurements of ballast samples collected at the field sites (see preceding section for sampling details). The following sections discuss the performance of various estimators. For Phase III of this project, ballast property estimators were made for the following properties and depth intervals:

1. Moisture in the 0–8-inch (0–20 cm) interval
2. Fouling in the 0–8-inch (0–20 cm) interval
3. Moisture in the 8–16-inch (20–40 cm) interval
4. Fouling in the 8–16-inch (20–40 cm) interval

If both the shallow and deep estimators indicated clean ballast, the ballast thickness could be inferred to be at least 16 inches (40 cm). If the shallow indicator returned a clean reading, and the deep returned a fouled reading, then the ballast thickness could be inferred to be approximately 8 inches (20 cm). It is possible to train estimators for deeper horizons, but the deep, multi-layer physical sampling was not conducted in the field outings due to limitations of manual sampling with a pickaxe and shovel.

4.2 Full Waveform Analysis

In Phase I of this project, researchers wrote a full-waveform modeling routine that numerically calculated received waveforms for bi-static GPR surveys over a layered subsurface (FRA, 2014). The team created an inversion algorithm to estimate layer properties, given GPR survey data, which they successfully tested with modeled data. Difficulties were encountered in attempting to invert RABIT data from in-service track because this data differed from the modeled data in several ways. First, when using ground-coupled antennas, the shape of the transmitted wavelet changed with changing material properties directly under the antenna. Additionally, there were NBVs that were not treated by an ideal layered subsurface model, listed in Table 6.

Table 6. Intrinsic and Non-Intrinsic Ballast Variations

Intrinsic Ballast Variations (IBVs)
Ballast minerology
Fouling materials type (e.g., breakdown, coal, or clay)
Non-intrinsic Ballast Variations (NBVs)
Ballast thickness
Sub-ballast properties
Graded or sharp boundary between ballast and sub-ballast
Rail height, rail wear, and tie plate seating
Cribs that are not completely full of ballast material, or are overflowing
Tie spacing and alignment
Tie condition (e.g., broken or waterlogged)
Timber ties versus concrete ties (concrete ties not yet studied)

For example, ties interfere with the direct wave transmission and change its shape. Since tie condition can be highly variable, it is difficult to properly model its effects. Initial attempts to use the full-waveform inversion approach were unfruitful. Because it would be difficult to properly treat all these situations in a physics-based model, this approach was abandoned in favor of other methods.

4.3 Waveform Attributes Analysis

Attributes of the waveforms recorded by the RABIT can be extracted and correlated to subsurface conditions. ESS used this approach in Phase I of this project (FRA, 2014) and results showed that some waveform attributes can be positively correlated with ballast fouling and moisture. Accordingly, ESS conducted an attributes analysis using the data collected in Phases II and III. The following waveform attributes were extracted from the RABIT field data described in Section 3. A second order polynomial fit was made between sampled ballast properties and the following attributes:

1. **Amplitude** is defined as the amplitude of the largest peak in the received waveform of either polarity.
2. **Arrival Time** is defined as the arrival time of the largest peak amplitude.
3. **Early Spectral Ratio** is defined as the spectral ratio using an early time window. Using a 16 ns time window centered about the time of peak arrival, calculate the ratio of the signal in the 500 to 750 MHz band to the signal in the 0 to 500 MHz band.
4. **Late Spectral Ratio** is defined as the spectral ratio using late time window. Using a 16 ns time window centered 8 ns after the peak arrival time, calculate the ratio of the signal in the 500 to 750 MHz band to the signal in the 0 to 500 MHz band.
5. **Weighted Attributes** are the above attributes weighted by their coefficient of determination (R value).

These attributes reflected the basic physics of radar wave propagation through ballast material according to the following assertions:

1. An increase in moisture content will increase the effective dielectric constant of the subsurface and cause the received energy to arrive later.

2. An increase in fouling material will also increase the effective dielectric constant of the subsurface and cause the received energy to arrive later.
3. An increase in contrast between the electromagnetic properties between the ballast aggregate and the void-filling material (i.e., air, water, and fouling material) will cause attenuation of the received energy, and this attenuation will be more pronounced at higher frequencies.

Phases I and II of this project noted that fouled ballast is heterogeneous and that one RABIT measurement at one location is not a representative sample. Therefore, from Phase II onward, RABIT ballast condition estimates have been made using measurements from 10 successive cribs. Accordingly, this approach was taken with the waveform attribute estimators. In Figure 10, the results of the polynomial fit are shown for the Group 4 (Topeka, KS, June 2018) field data, and Figure 11 shows the predicted properties using polynomials fitted to field data Groups 1–4. Data from Group 5 (TTC near Pueblo, CO) was not included because there may have been issues with the instrument response during this field outing (see Section 3.6 for details). The team investigated the performance of the attributes method using a single training group and using multiple groups to determine if this method was training on location specific features. The Group 4 results were better than the results for Groups 1–4, indicating that over-fitting to site-specific conditions may occur when training with overly localized data. The poor performance of the ballast property estimators fitted to multiple field data groups indicated that these simple, attribute-based estimators were insufficient for application over a wide variety of track conditions. Likely, location-specific NBVs (such as ballast thickness, sharp or graded boundary between ballast and sub-ballast, crib over/under filling, rail height, etc.) cause variation in the measured RABIT waveforms that cannot be accounted for in this simple attribute-based model.

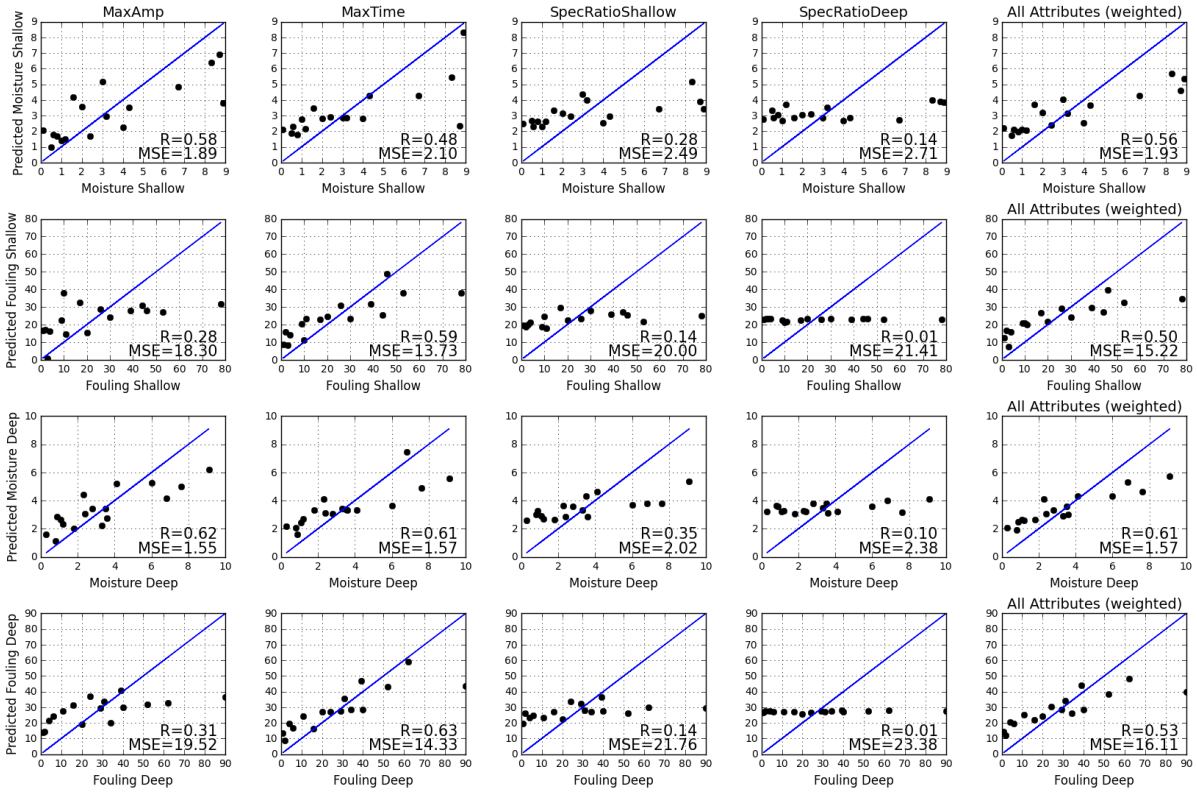

Figure 10. Predicted ballast properties using waveform attributes from field data Group 4 (Topeka, KS, June 2018)

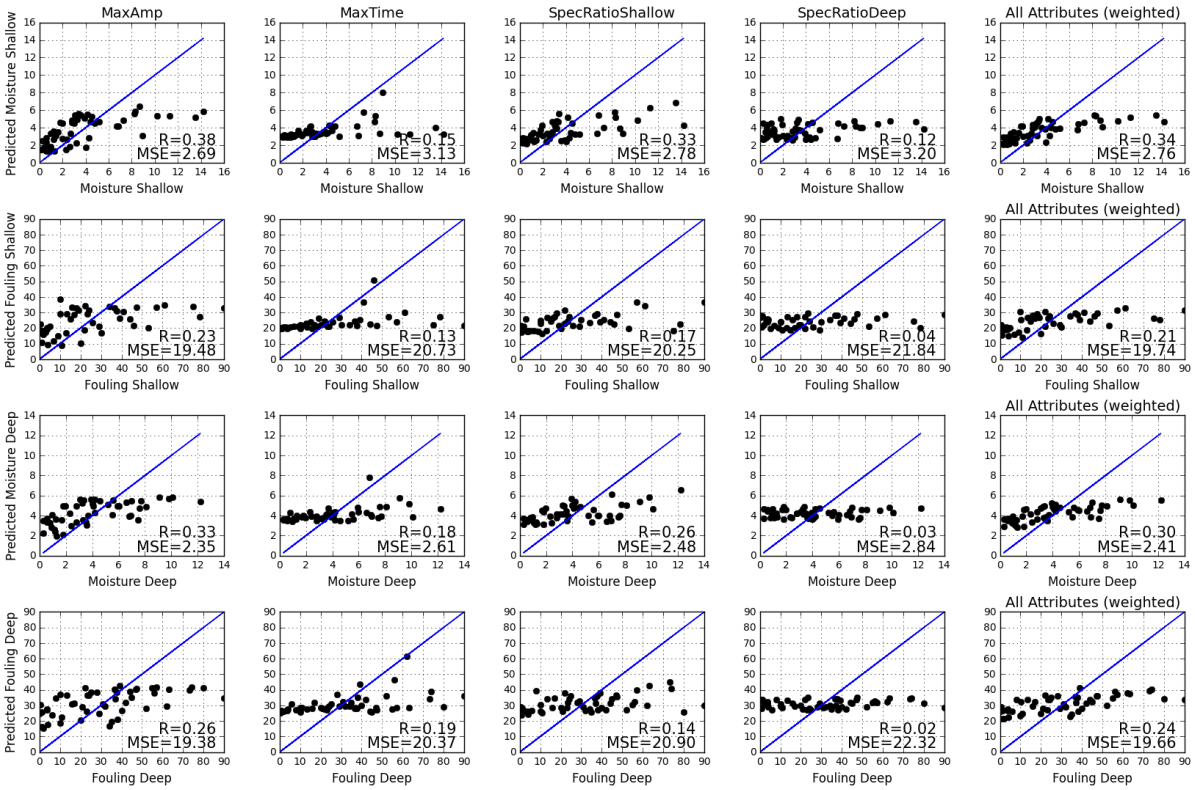

Figure 11. Predicted ballast properties using waveform attributes from data groups 1–4

4.4 Neural Network Analysis

As mentioned in the previous section, measurements taken at a single location (i.e., a spot measurement) on a track are not likely to be representative of the average properties in the local area (as demonstrated in Phase I of this project). The variability in the RABIT data collected for this project indicated that both physical variations in ballast properties and NBVs were likely occurring at adjacent locations along a track. Neither the physics-based algorithms for estimating ballast properties created in Phase I nor the waveform attributes-based analysis from the previous section accounted for these NBVs. For example, Figure 12 shows variability in tie spacing and alignment observed on the test track. Tie alignment is one of many NBVs the analysis algorithm should tolerate. Specifically, an algorithm to estimate ballast properties should tolerate changes in NBVs, such as:

1. Ballast mineralogy
2. Ballast thickness
3. Sub-ballast properties
4. Fouling materials type (e.g., breakdown, coal, clay)
5. Graded or sharp boundary between ballast and sub-ballast
6. Rail height, rail wear, and tie plate seating
7. Cribs that are not completely full of ballast material or are overflowing
8. Tie spacing and alignment

9. Tie condition (e.g., broken or waterlogged)
10. Timber ties versus concrete ties (concrete ties not yet studied)

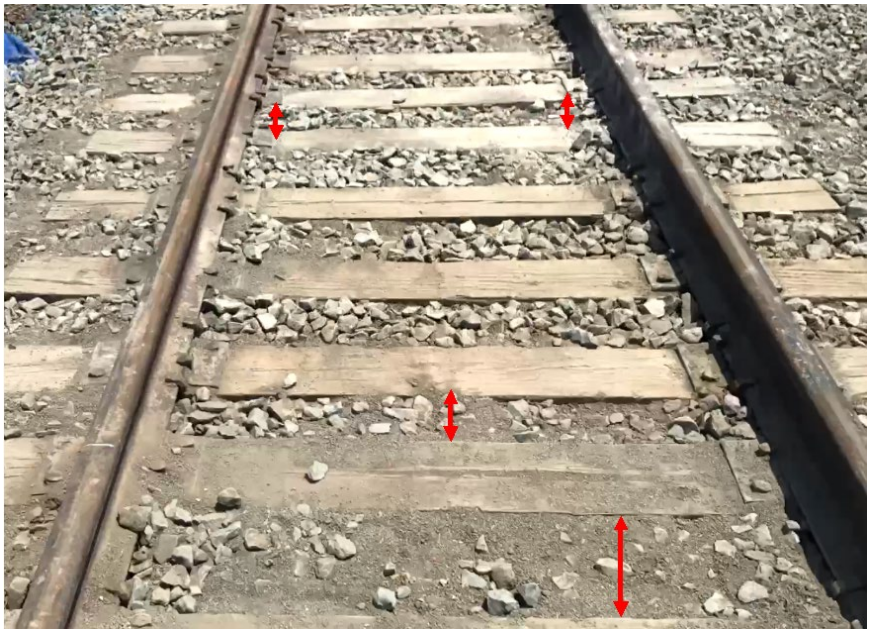

Figure 12. Variable tie spacing and alignment observed on the test track

Neural networks, however, are known for their ability to recognize complex patterns in data (e.g., speech and handwriting recognition) and are a good choice for creating ballast property estimators that are tolerant to noisy environmental variations. Neural network estimators must be trained using training data and then validated using independent test data. In this work, a subset of the data collected from the field outings was used to train various neural networks, and the remaining data were used to validate the performance of the networks. The details are covered later in this section.

As noted previously, changes in ballast properties cause changes in waveform attenuation and propagation time. To optimize the performance and training of the neural network, the team pre-processed the GPR data so that changes in attenuation, propagation velocity, and changing properties with depth were clear. They accomplished this by selecting A-scans corresponding to when the RABIT was centered over a tie (Figure 1). Then, they calculated a spectrogram to provide a representative image of the waveform (Figure 13). Each pixel of a spectrogram indicates how much energy the waveform has at a certain frequency and arrival time. These spectrogram pixels form a rich set of waveform attributes that the neural network can correlate with ballast properties. The challenge is to train the neural network by reinforcing accurate performance so that it provides accurate results in a wide variety of site conditions without over-training it on local site-specific conditions. A separate neural network was trained for each ballast property/depth combination for a total of four networks. For the shallow neural networks, training data were limited to the first 10 ns of spectrogram data, and the deep network was trained with the final 15 ns of data. This temporal division was selected based on the configured acquisition system hold-off time, typical shallow travel times for different ballast materials (~3–6 ns), and period of the transmitted wavelet (~2 ns). This provided 260 input data values (or attributes) for the shallow estimator and 390 values (or attributes) for the deep estimator.

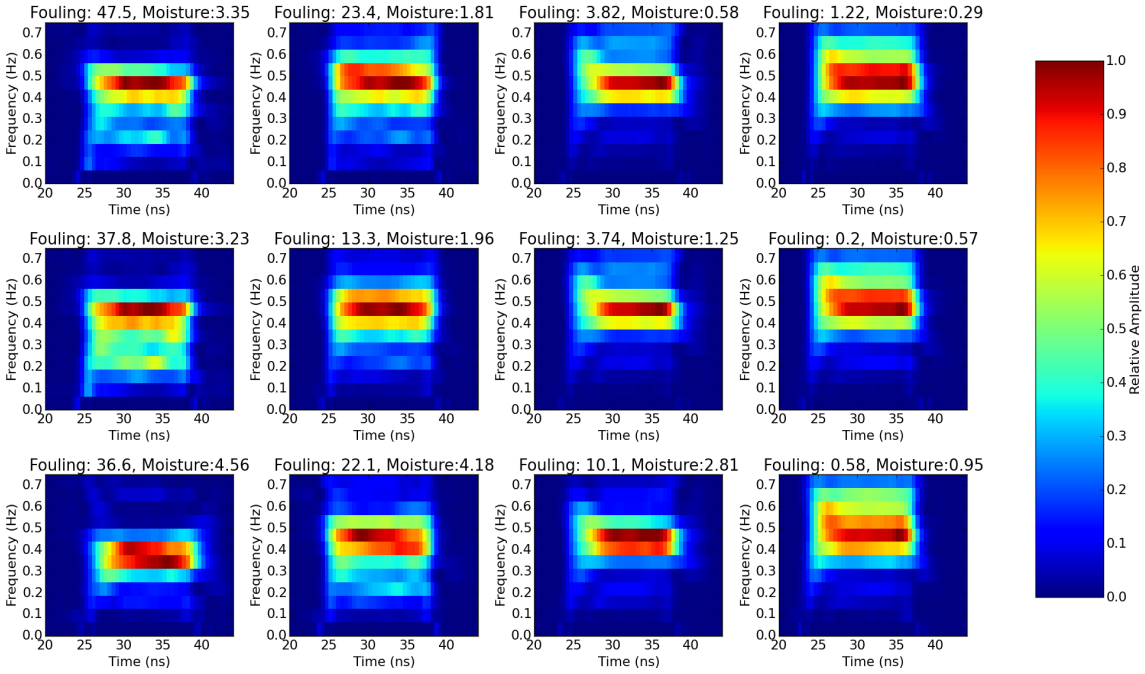

Figure 13. Spectrograms generated from selected A-scans were used as inputs to the MLP.

The multi-layer perceptron (MLP) network topology (Figure 14) works well for stationary image classifiers that must recognize complex patterns in the data. ESS selected a four-layer MLP for this problem, with 260 or 390 inputs (one for each pixel in the spectrograms), a first hidden layer (260 or 390 perceptrons), a second hidden layer (128 perceptrons), and two output stages: one for moisture estimation and the other for fouling. The output of each perceptron used a rectifier function where positive values are unchanged and negative values are zero. Two hidden layers were used so the network could make complex decisions with sufficient accuracy (see Table 7 for more information). The training phase used the spectrograms from RABIT measurements taken on the right side of the track for each tie of each site of each field data group. Each network was trained for 1,000 epochs. After training, the weighting coefficients were determined for each perceptron and the network could then be used as an estimator. Consult Géron (2017) and Hagen, et al. (2014) for more details on the architecture and training of neural networks.

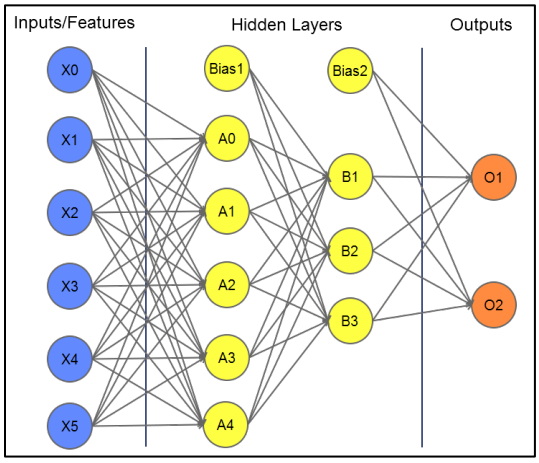

Figure 14. A four-layer MLP

Table 7. Capability of Neural Networks (Heaton, 2008)

No. Hidden Layers	Capability
0	Only capable of representing linear separable functions or decisions
1	Can approximate any function that contains a continuous mapping from one finite space to another
2	Can represent an arbitrary decision boundary to arbitrary accuracy with rational activation functions and can approximate any smooth mapping to any accuracy

4.5 Neural Network Training and Verification

The neural networks were trained with several datasets. The first training dataset was comprised of all the RABIT data from the right rail from field data Groups 1–4 (with 646 waveforms from 646 tie locations at 67 sites). The results are shown in Figure 15. The Group 5 data were omitted from this training group because the RABIT response from this data group was suspect. The predicted data were generated using the RABIT data from the left rail in the same field data groups. In Figure 15, the first and third rows show the predicted ballast properties using data from each tie, and the second and fourth rows show the predicted values averaged over all RABIT measurements at a test site (i.e., averaged over 10 ties—see circled data points). The acquisition procedure was to collect data with the RABIT straddling 10 adjacent ties at each test site. Variations in the received waveforms from side to side and from crib to crib were evident (see Figure 4 through Figure 8). Taking the average of the predicted values over 10 adjacent ties improved the correlation and mean-squared error (MSE) between the predicted and the measured values. This averaging produces a more representative estimate that is not overly sensitive to single crib ballast conditions or NBVs (see Table 8). Next, a set of networks was trained using all the GPR data from the right rail from field data Groups 1–5 (with 916 waveforms from 916 ties locations at 94 sites), and the results are shown in Figure 16. Even though the data from field Group 5 were suspect, including these data into the training set did not reduce the accuracy of the neural network estimators.

The previous results in Figure 15 and Figure 16 were obtained using data collected on the right rails (gage side) to train a set of networks and data collected on the left rail (gage side) to test them. Although Figure 5 through Figure 9 (see Section 3) illustrate that there was significant variation from one side of the track to the other, it was likely that the NBVs did not change much across a given test site. However, the NBVs likely did change significantly across different field data groups. To examine these effects, a set of networks was trained using right rail data from field Groups 1–3 and another set trained from right rail data from Groups 1–4 (see Table 9). Then the performance of these networks was tested using left rail data from Group 4. When data from the Group 4 location were not included in the training data, the MSE for fouling increased from about 6 percent to 16 percent, and the MSE for moisture increased from about 1 percent to 2.5 percent. Similar results were obtained when excluding Group 3 data from training (see Table 9). The estimator results for locations not used in training still had useful accuracy, but the MSE was 2–3 times greater than with estimators for which test locations had been included in the training data. The ballast and fouling material were of similar makeup (i.e., granitic) in all the test locations, so the most plausible explanation of the different estimator accuracies was that there were NBVs at the excluded group locations that had not been incorporated into the training. Alternatively, the networks may have been over-training on NBVs from the included training locations. This supported the following well-known recommendations for neural networks: 1) the training dataset should be sufficiently diverse to include the expected range of variations, and 2)

the training dataset should be large enough to prevent over-fitting on specific examples. Over-fitting occurs when the neural network has so much information processing capacity that the limited amount of information contained in the training set is not enough to train all the neurons in the hidden layers (or that there are too many neurons for the limited training data).

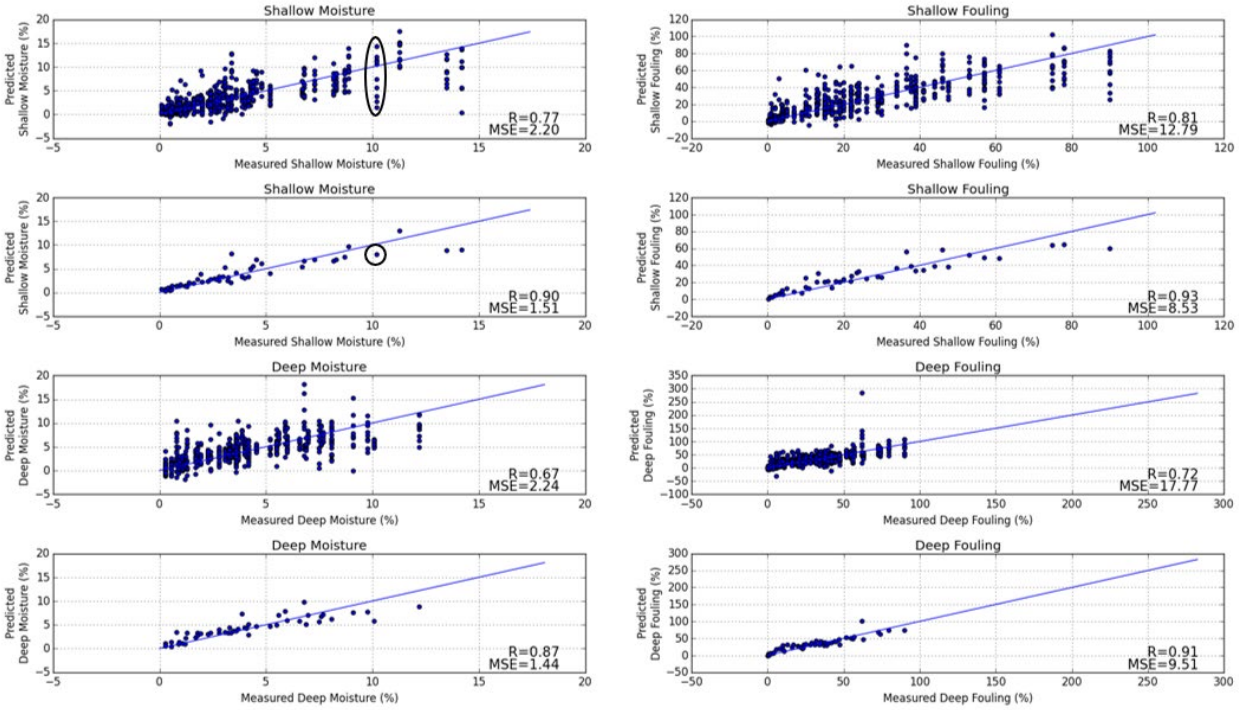

Figure 15. The graphs show predicted moisture and fouling from a neural network trained on field data groups 1–4 versus measured values obtained from physical sampling. The first and third rows show the predicted ballast properties using data from each tie, and the second and fourth rows show the predicted values averaged over all RABIT measurements at a test site (i.e., averaged over 10 ties—see circled data points).

Table 8. Investigating performance without localized training

Training Groups	Test Group	Property	MSE	R
1, 2, 3	4	Shallow Moisture	2.70%	0.75
		Shallow Fouling	15.47%	0.75
		Deep Moisture	2.47%	0.70
		Deep Fouling	18.17%	0.72
1, 2, 3, 4	4	Shallow Moisture	0.75%	0.97
		Shallow Fouling	5.51%	0.97
		Deep Moisture	1.02%	0.93
		Deep Fouling	8.14%	0.94
1, 2, 4	3	Shallow Moisture	1.67%	0.81
		Shallow Fouling	7.08%	0.90
		Deep Moisture	2.43%	0.50
		Deep Fouling	13.98%	0.61
1, 2, 3, 4	3	Shallow Moisture	0.57%	0.97
		Shallow Fouling	4.44%	0.96
		Deep Moisture	1.71%	0.74
		Deep Fouling	8.95%	0.80

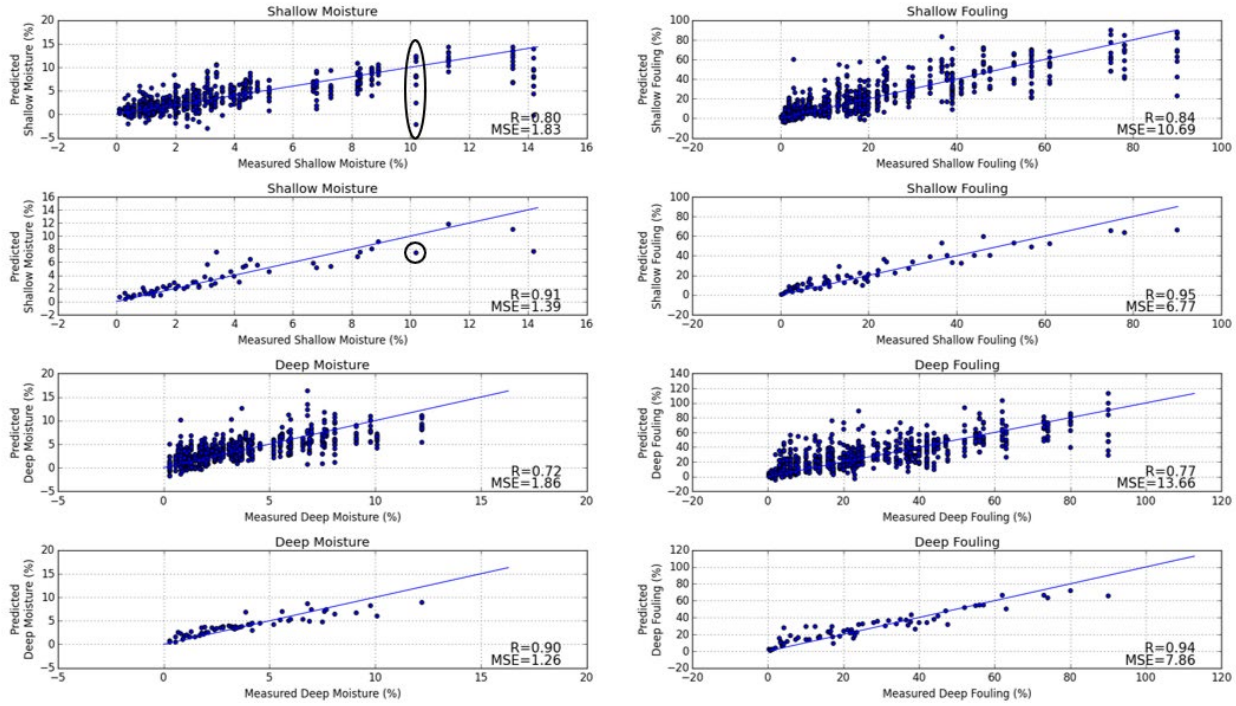

Figure 16. The graphs show predicted moisture and fouling from a neural network trained on field data groups 1–5 versus measured values obtained from physical sampling. The first and third rows show the predicted ballast properties using data from each tie, and the second and fourth rows show the predicted values averaged over all RABIT measurements at a test site (i.e., averaged over 10 ties—see circled data points).

The neural network estimators created in this work can likely tolerate most of the variations listed in the first paragraph of this section with some exceptions. First, concrete ties and their rebar will likely affect the GPR response, and separate training datasets and estimators will likely be needed for use with concrete ties. Second, the electromagnetic properties of both coal and dust from ballast breakdown are similar; however, clay minerals can have significantly different properties. There are many different types of clay minerals with different electromagnetic properties, and some are sufficiently different that they would require specially trained estimators.

4.6 Relationship between Moisture and Fouling

It is the fine-grained component of fouled ballast that holds moisture; a given amount of moisture implies at least a certain amount of fouling. Per FRA data from Phase I (2014), the field capacity (i.e., the maximum amount of water that can be held) of fouled ballast is about half of the fouling percentage by volume, or about one-fourth of the fouling percentage by weight. Figure 17 plots moisture versus fouling for physical samples taken from the field data groups. The dashed line is the 1:4 ratio described above. Most of the samples fall below this line, and it is likely that those that do not are from locations where a thunderstorm had recently passed, as this happened several times throughout field testing.

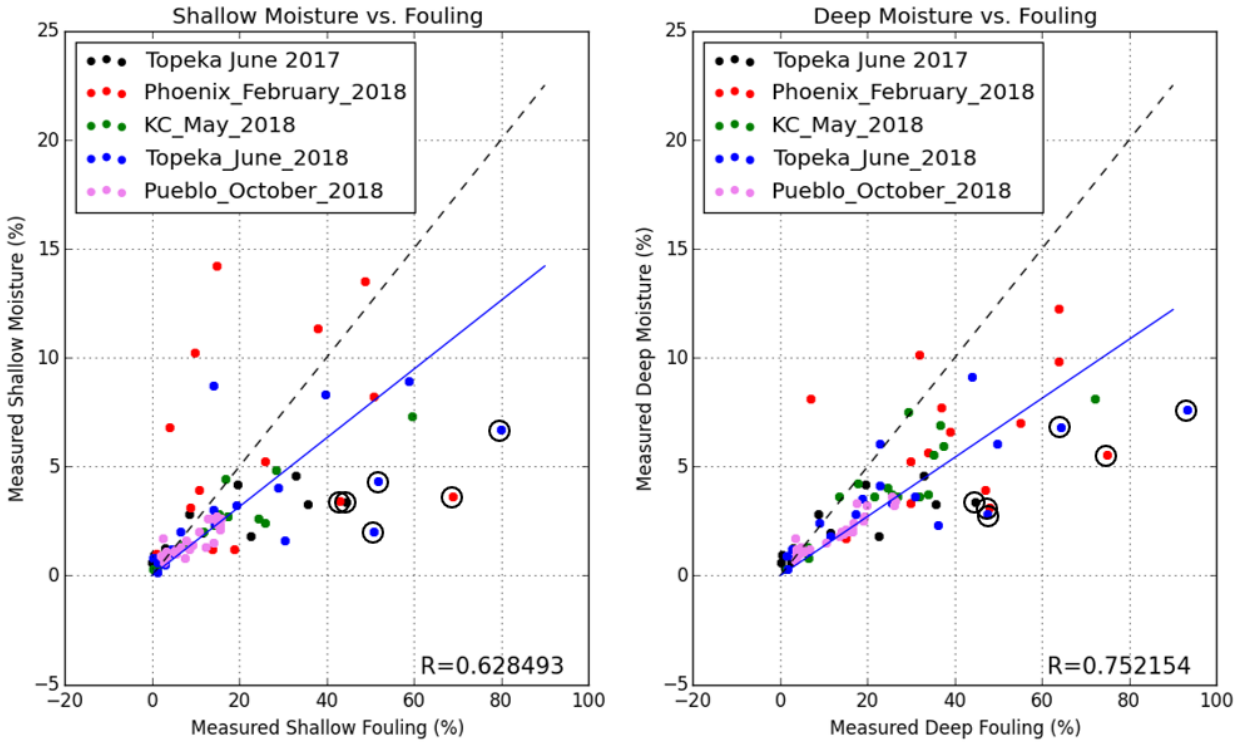

Figure 17. Graphs show moisture versus fouling from physical samples taken from in-service track. Dashed line is field capacity and blue line is the linear regression.

The R-values in Figure 15 indicate that there was a significant correlation between fouling and moisture. However, the field capacity studies indicate the reverse is not true: high fouling levels do not imply high moisture levels. ESS selected data from the test site locations with a high fouling index and low moisture to test if the neural network could properly distinguish fouling from moisture (see six circled data points in Figure 15). Moisture and fouling were estimated using the RABIT data from the left rail at these six site locations and the network was trained with right-rail data from field data Groups 1–4 (see Figure 18 and Figure 19). Although the sample size was small, the estimated moisture values were considerably less than the values that would be predicted using the field capacity or linear regression lines in Figure 15. This supported the conclusion that the neural network had learned to distinguish moisture from fouling. Note that with such a small sample size (n = 6), the accuracy of the R and MSE statistics was low—hence the variability seen in Figure 18 and Figure 19. Although this result is encouraging, more testing on field sites with low moisture levels and high fouling levels are needed to further test and reinforce this conclusion.

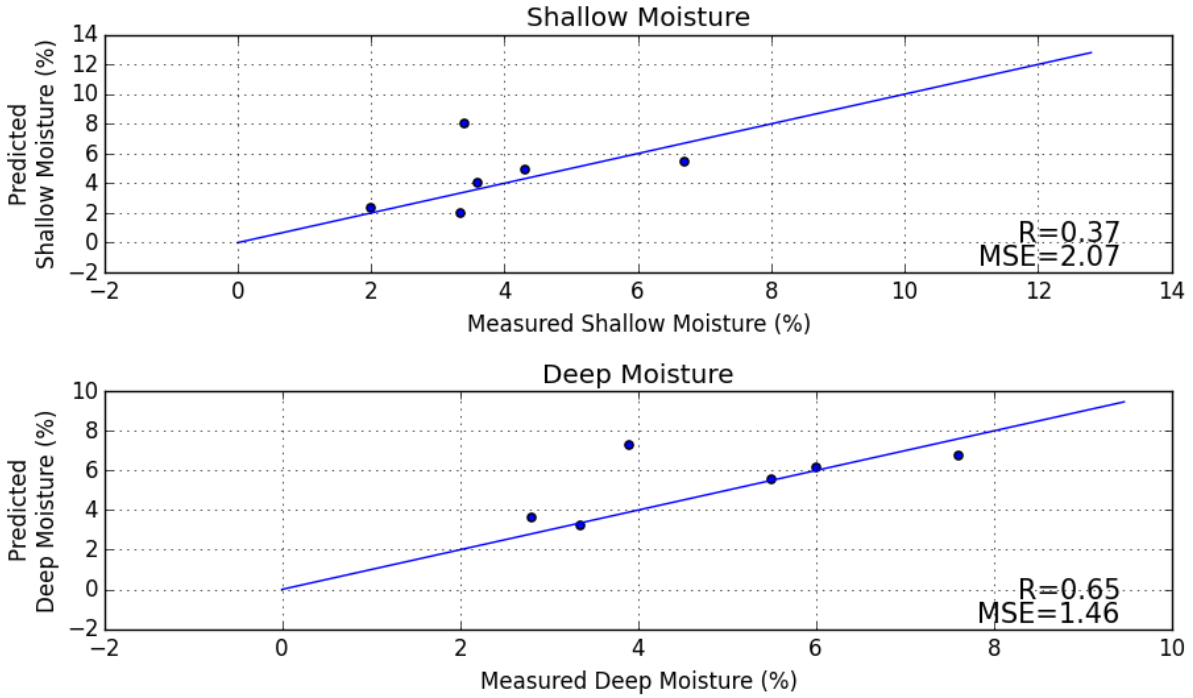

Figure 18. Predicted moisture for locations with a high fouling index and low moisture content

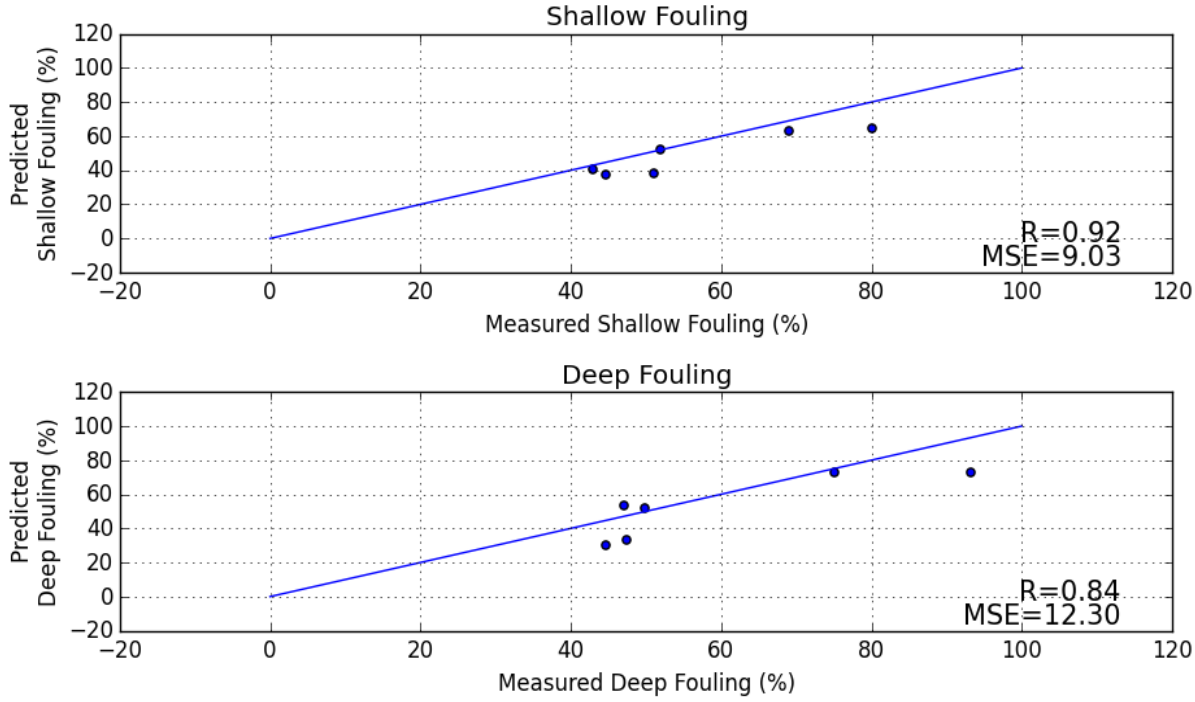

Figure 19. Predicted fouling for locations with a high fouling index and low moisture content

5. RABIT User Perspective

The following sub-sections give a step-by-step overview of the operation of the RABIT for conducting an inspection survey. An FRA Regional Track Inspector conducted an independent evaluation of the usability and portability by an FRA regional track inspector; this section includes proposed improvements based on this feedback.

5.1 Conducting a Survey

When conducting a survey, users follow the steps outlined below. Figure 20 shows a screenshot of the acquisition software. The upper part of the screen shows the GPR waveforms, and the lower part shows the estimated ballast condition for the 0–8-inch (20 cm) depth interval (top) and the 8–16-inch (20–40 cm) depth interval (bottom). Users can also generate a report summarizing the results (see Figure 21). Note that each survey is tagged with a location from the onboard GPS unit. A user manual is available with more information on these screens and operation of the unit.

RABIT Survey Procedure:

1. Remove the unit from the shipping case, assemble the outrigger, and place it on the track.
2. Power up the RABIT and MS Windows 10 tablet computer, then start the acquisition program on the tablet. After about a minute, the software will have initialized and connected to the RABIT.
3. To make a ballast measurement, the user will turn on data recording, position the RABIT at the site of interest, then press the "mark" button. This process is repeated 10 times with the RABIT positioned at the next tie so that a representative volume can be measured.
4. Finally, the software will analyze the data collected at the last 10 positions and display the estimated moisture and fouling levels. A report can be generated with the results.

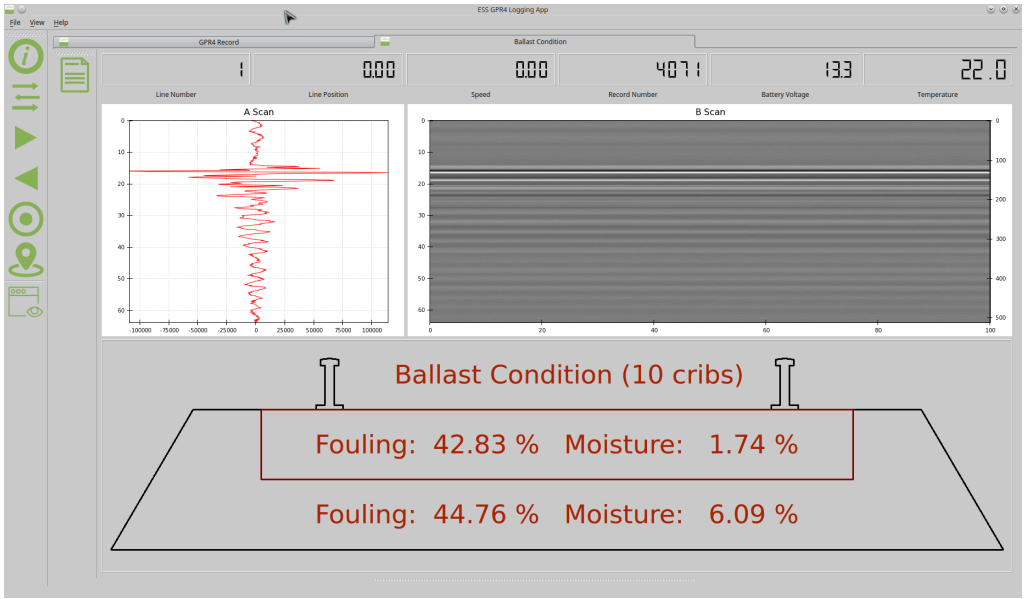

Figure 20. The screenshot from data acquisition and analysis software shows moisture and fouling estimates from in-service track.

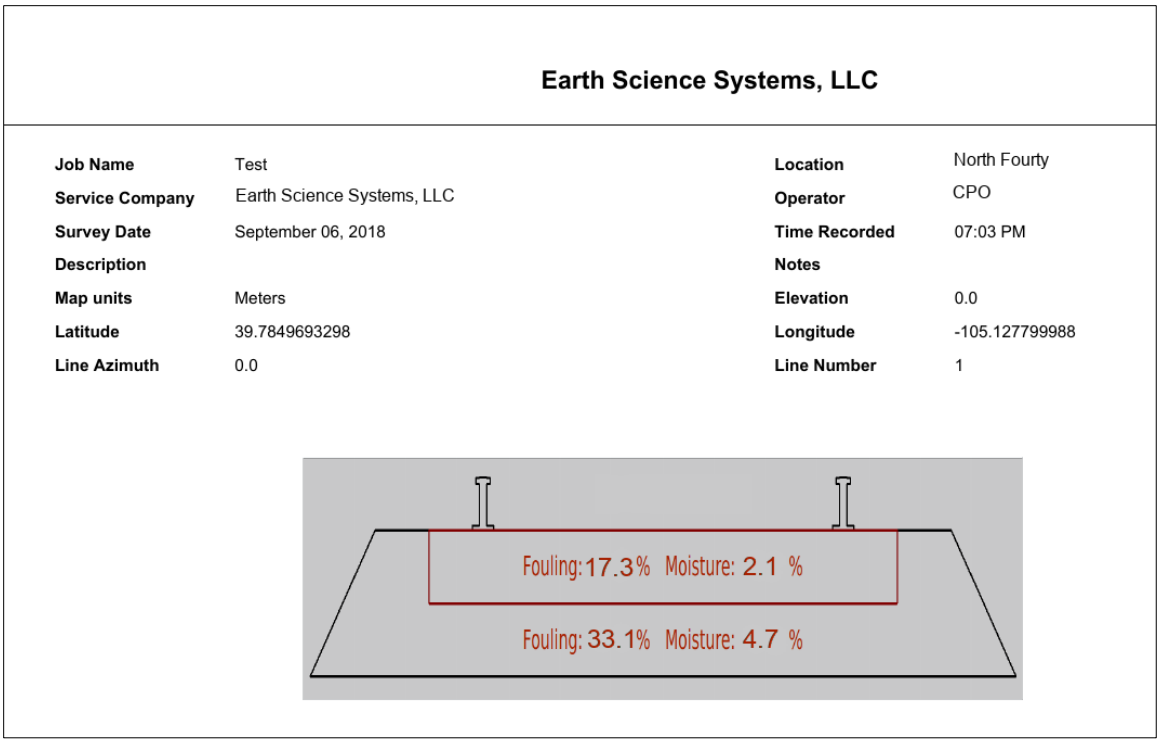

Figure 21. Sample report generated by analysis software

5.2 FRA Inspector Feedback

The RABIT went to an FRA Office of Safety Region 7 Track Inspector for an independent evaluation. The inspector operated the unit and evaluated its usability and portability. His report can be summarized as follows:

1. The RABIT has great capabilities.
2. The RABIT is easy to use and lightweight.
3. The software is easy to use.
4. The estimated ballast properties appear to be accurate (but the only comparison was with a visual inspection).
5. The shipping case is much too large, and transport by a single person is difficult (see Figure 22). This needs to be addressed because inspectors usually travel alone.
6. The RABIT was designed for use on 132-lb AREA rail (rail height: 7 1/8 inches), 136-lb AREA rail (rail height: 7 5/16 inches), or 141-lb AREA rail (rail height: 7 5/8 inches), which give a clearance of 3.25 to 3.75 inches. When tested on shorter rail heights, the device could not be rolled along the track because the device rested on the antennas rather than the wheels. Adjusting the rail height would allow the system to be used on rail lines with shorter rail heights (e.g., shortline railroads) rather than just Class I railroads.

Figure 22. RABIT system in its current shipping case

5.3 RABIT Improvements

The current RABIT system is the result of several cycles of engineering and testing over the course of the project. Nevertheless, as testing progressed and more users provided feedback, areas for improvement came to light. The current recommended improvements are list below:

1. Although the size and weight of the RABIT has been reduced, its shipping case is still too heavy and bulky. This was the primary issue raised by an FRA inspector. To reduce the size of the case, a new frame design has been planned so that it can be disassembled and packaged in a significantly smaller shipping case.
2. The current RABIT was designed for the large rail sizes used in Class I railroads, and the height cannot currently be adjusted. The new frame design will allow a height adjustment.
3. During the last few years of the RABIT project, ESS has made improvements to its GPR technology and is currently introducing new commercial GPR systems. These new systems contain some electronic improvements to increase the fidelity of the signal which have not yet been added to the RABIT system. Although these changes will improve the system response, to date, the research team has refrained from making these changes because data with a different system response could be difficult to merge with the existing dataset.

4. The system has not yet been FCC certified. This is legally required when conducting commercial services using the instrument (i.e., if it were sold as a unit or used as a service) because the device emits radio frequency energy.
5. Additional RABIT surveys on rail lines and collection of ballast samples for ground truth are needed to build a more diverse training dataset for the neural network algorithms.

6. Finite Element Modeling

One of the goals of this project is to make a connection between ballast condition and ballast behavior (i.e., ballast strength). To address this goal, ESS researchers built a finite element model (FEM) using the track and ballast geometry of the test track at the BNSF Technical Research and Development facility in Topeka, KS. The team originally planned to use the FEM modeling packages ANSYS and GeoTrack to determine the characteristics of the track system under load, but they ultimately used COMSOL Multiphysics due to user familiarity. The team made a 3-dimensional model of a 15-foot (5-meter) section of track based on measurements taken at the BNSF site. The model was a linear elastic structural mechanics model that could calculate deformation and stress conditions based on a loading input. The model was designed to apply one axle load on the rails at the center of the track and assumed a static loading condition. These models required the physical dimensions and the elastic properties of ballast. The modulus values were obtained from lightweight deflectometer (LWD) readings taken at the test track. Figure 23 shows the modeled deflection due to axle loads of 28 and 39 tons. The modeling framework built for this simulation can be extended to help predict ballast behavior at other sites using field observations.

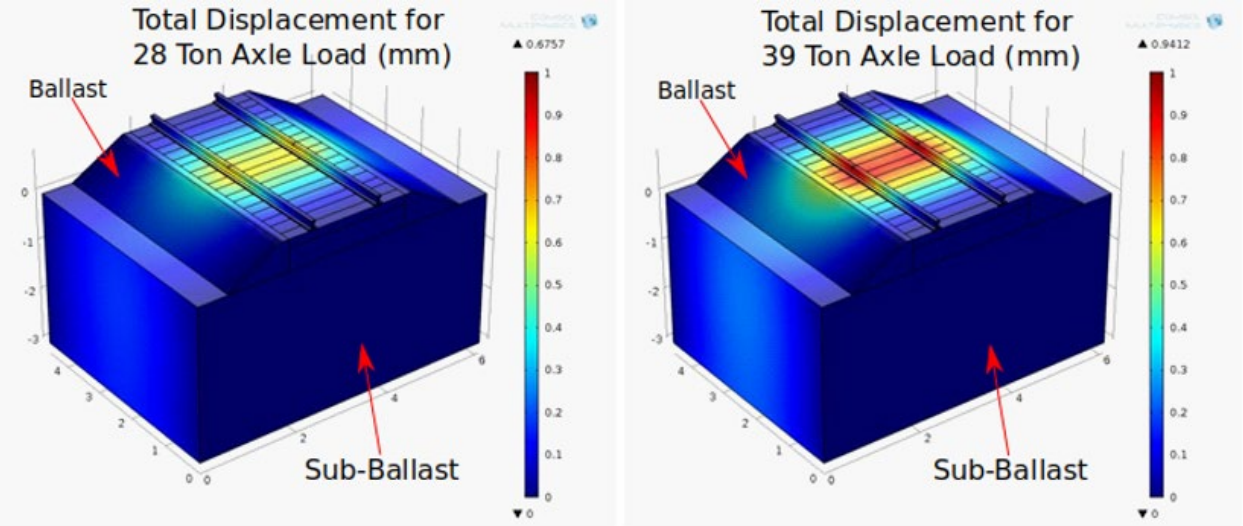

Figure 23. The figure shows FEM modeling results for the test track at the BNSF research facility in Topeka, KS. Geometry units are meters and displacement is in mm. Ballast is 2 feet (60 cm) thick.

After the data were collected from the Phoenix, AZ sites, the COMSOL model was updated to more closely mirror the geometry measured in the field. Figure 24 shows the geometric model used in the analysis and typical output results. The team selected three locations in the Phoenix area for modeling of geometric data, LWD, deflection measurements, and ballast moisture. These locations were tested before and after a heavy rain, allowing the same section of track to be tested when dry and partially saturated. Ballast samples collected after each round of testing provided a moisture content measurement. Table 9 summarizes the modeled locations and the corresponding ballast condition.

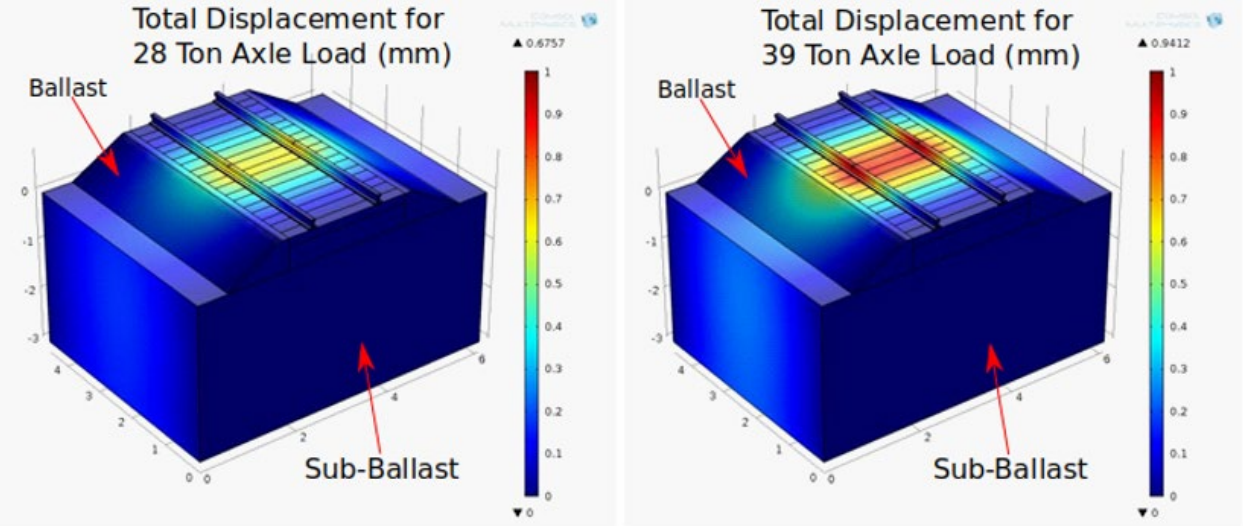

Figure 24. The figure shows the geometry of the Phoenix, AZ test site track (left) and an example of displacement due to load (right). Geometry units are meters and displacement is in mm. Ballast is 2 feet (60 cm) thick.

Table 9. Fouling and moisture values from the Phoenix test sites. Sites 10–12 were at the same locations as sites 1–3 but were sampled after a rain event.

Site	Water Content (%)	Fouling (%)	LWD Modulus (ksi)	Measured Deflection (in [mm])	Modeled Deflection (in [mm])
1	4.4	21.5	12.9	0.250 (6.4)	0.0313 (0.797)
2	3.7	45.0	14.2	0.375 (9.5)	0.0305 (0.776)
3	5.3	25.0	14.7	0.438 (11.1)	0.0302 (0.769)
10 (1)	9.0	23.5	11.8	0.281 (7.1)	0.0321 (0.817)
11(3)	12.1	23.5	12.8	0.469 (11.9)	0.0315 (0.799)
12 (2)	9.2	46.5	12.3	0.375 (9.5)	0.0317 (0.806)

Although there is a general positive correlation between moisture, modulus, and measured deflection, the ballast modulus measured by the LWD did not always correlate to the measured deflections or to the physical conditions of the ballast (i.e., fouling and moisture). Furthermore, the modeled deflection was significantly less than the observed deflections in the field. Possibly, the magnitudes of the measured rail deflections depended more on the mechanical connections between the rail and ties than the interactions between the ties and ballast. Another possibility is that the ballast material was not homogenous with respect to modulus and that the ballast below the ties could have been lower than the modulus measured by the LWD from the surface between the cribs. One advantage of the RABIT is that it can make deeper measurements than the LWD, which could provide insight into this hypothesis. One final consideration was that the loading observed in the field included a rebound unloading cycle that lifted the rail above the original position before a subsequent loading cycle. The deflection measurements only measured the offsets that occurred in the direction of the earth and did not measure the magnitude of the rebound effects. Also unknown was whether the bottom of the ties remained in contact with the ballast throughout the loading cycle.

Given the available information and based on the model results and observed field conditions, it was not possible to conclude precisely why the observed behavior in the field was of a

magnitude so much larger than that seen in the model results. Researchers may learn more by capturing deflection measurements with more precise equipment (e.g., LVDT gages, multi-depth deflectometers) and on more elements than under the rail mid-crib.

7. Conclusion

For this project, the research team designed, built, tested, and evaluated a second-generation GPR ballast inspection system. This system provides a non-invasive method to estimate the amount of fouling and moisture present in in-service track in real time. The results showed that fouling and moisture estimates correlated well with actual values (mean-squared-errors of 1.39 for moisture and 7.86 for fouling) when results were averaged over 10 ties.

Although the system is portable, it could be improved in multiple ways. The system is too bulky to be easily transported in the field, as outlined in Section 5.3. The shipping container needs to be much smaller, and the frame could be redesigned to collapse for packing into a smaller shipping container. The frame should be adjustable so that it supports multiple rail heights, not just Class I railroads. The electronics should be updated to the latest, high-fidelity electronics used in other production ESS GPR systems. Finally, the system requires FCC certification before it can be used on any commercial work (i.e., sold as a unit or used as a service).

GPR data analyses to estimate ballast properties can be accomplished with several methods. Analyses based on full-waveform modeling and inversion are impractical because there are many environmental effects not associated with ballast properties that affect the radar waveforms, and it would be difficult to accurately model all of them. Based upon the results obtained in this study, analyses based on waveform attributes were possible, but uncertainties in the estimated ballast properties were high, and the method likely needs to be calibrated for each locale. Analyses based on neural networks provided robust estimates with low uncertainties. The results thus far indicated that this approach could tolerate environmental variations not associated with ballast properties, but additional testing in more varied environmental conditions is needed to support this conclusion.

Further field testing will provide two related benefits. First, it will provide a more diverse training dataset that will enable accurate ballast property estimates in a wider variety of environmental conditions; second, further field testing can help verify that the RABIT provides accurate estimates over a wide range of conditions. Throughout the course of this project, researchers conducted field testing at 94 sites in 3 regions (Phoenix, AZ; Topeka and Kansas City, KS; and Pueblo, CO). Certainly, there are environmental differences between these three regions and between different sites within each region. Sites for further field testing should be selected such that they: 1) are from different parts of the country, 2) have different ballast thicknesses, 3) have different gradations between ballast and sub-ballast, 4) have different rail heights, and 5) have different tie plate sizes, etc.

There are other promising neural network topologies, such as convolutional neural networks and recurrent neural networks. Other training methods can also be employed to ensure that the network is not over-fitting the training data. One method for accomplishing this is to “forget” or “blur” some knowledge at interim training iterations and wait for this knowledge to be reinforced by subsequent training iterations. Researchers may investigate these approaches if the current routines are failing at some test locations that are not markedly different environmentally from the training environments.

From first principles, the current estimators should provide reasonable results when the fouling material is ballast breakdown, sand, or coal, because these materials have similar electromagnetic properties as ballast aggregate material (e.g., granite). Ballast with clinkers will

be problematic due to the unusual electromagnetic properties of clinkers. Fouling by mineralogic clay minerals will also be problematic due to their widely varying electromagnetic properties. No problems are anticipated when fouling occurs with non-mineralogical clay (i.e., very fined-grained material without a high concentration of clay minerals). All testing to date has been conducted on track with timber ties. Concrete ties with rebar will likely change the GPR waveforms, and operation in this environment needs to be studied.

In a short study, the team attempted to connect ballast properties to ballast behavior and performance. They measured moisture, modulus, and rail deflection at a few field sites near Phoenix, AZ, and these measurements showed a positive correlation between the measured properties. The team created a finite element model that reflected the geometry of the track at these sites, but the modeled deflections did not accurately reflect the measured deflections. This type of modeling would be a valuable tool for predicting track substructure performance, but the time and resources available for this task were too limited for this project. The research team recommended investigating the relationship between fouling, moisture, and modulus. With this knowledge, researchers can map ballast fouling and moisture measurements to predicted modulus values and the substructure performance predicted through FEM modeling.

8. References

Al-Qadi, I., Wie, X., and Roberts, R. (2007, January). *Scattering Analysis of Railroad Ballast Using Ground Penetrating Radar.* Transportation Research Board Annual Meeting, Washington, D.C.

ASTM International. (2007). *Annual Book of Standards, Volume 04.08, Soil and Rock (1): D420 - D4914.* ASTM International, Philadelphia, PA.

ASTM International. (2008). *Annual Book of Standards, Volume 04.08, Soil and Rock (II): D5714 – Latest*. ASTM International, Philadelphia, PA.

Federal Railroad Administration. (2014). *Final Report for FRA-TR-010: Ballast Fouling Measurement Tool – Phase I.* (DOT/FRA/ORD-18/33). U.S. Department of Transportation.

Géron, A. (2017). *Hands-On Machine Learning with Simit-Learn and TensorFlow.* O'Reilly Media, Inc., Sebastopol, CA.

Hagan, M.T., Demuth, H.B., Beale, M.H., and De Jesús, O. (2014). *Neural Network Design* (2nd ed.). Oklahoma State university, Stillwater, OK.

Heaton, J. (2008). *Introduction to Neural Networks for Java* (2nd ed.). Research, Chesterfield, MO.

Oden, C. P. (2006). *Calibration and Data Processing Techniques for Ground Penetrating Radar Systems with Applications in Dispersive Ground* (Doctoral dissertation). Colorado School of Mines, Golden, CO.

Powell, W.D., Potter, J.F., Mayhew, H.C., and Nunn, M.E. (1984). *The Structural Design of Bituminous Roads* (LR 1132). Transport and Road Research Laboratory, Crowthorne, Berkshire, U.K.

Rubin, A. J., Ho, C. L., and Oden, C. P. (2018). *A Comparison of Railroad Ballast Elastic Modulus as Estimated from Lightweight Deflectometer (LWD) and Dynamic Cone Penetrometer (DCP).* Transportation Research Board Annual Meeting, Washington DC.

Selig, E. T., and Waters J. M. (1994). *Track Geotechnology and Substructure Management.* T. Telford, London.

Silvast, M., Nurmikolu, A., Wiljanen, B., and Levomaki, M. (2010). An Inspection of Railway Ballast Quality Using Ground Penetrating Radar in Finland. *Proceedings of the Institution of Mechanical Engineers, Part F: Journal of Rail and Rapid Transit, 224*(5), 345–351. DOI 10.1243/09544097JRRT367.

Yoo, T. S., Chen, H. M., and Selig, E. T. (1978, March). Railroad Ballast Density Measurement. *Geotechnical Testing Journal, 1*(1), 41–54.

Abbreviations and Acronyms

ACRONYM	DEFINITION
EM	Electromagnetic
ESS	Earth Science Systems, LLC
FCC	Federal Communications Commission
GPR	Ground Penetrating Radar
FRA	Federal Railroad Administration
LVDT	Linear Variable Differential Transformer
MSE	Mean Squared Error
MLP	Multi-Layer Perceptron
RABIT	RAdar Ballast Inspection Tool
TTC	Transportation Technology Center
UMass	University of Massachusetts